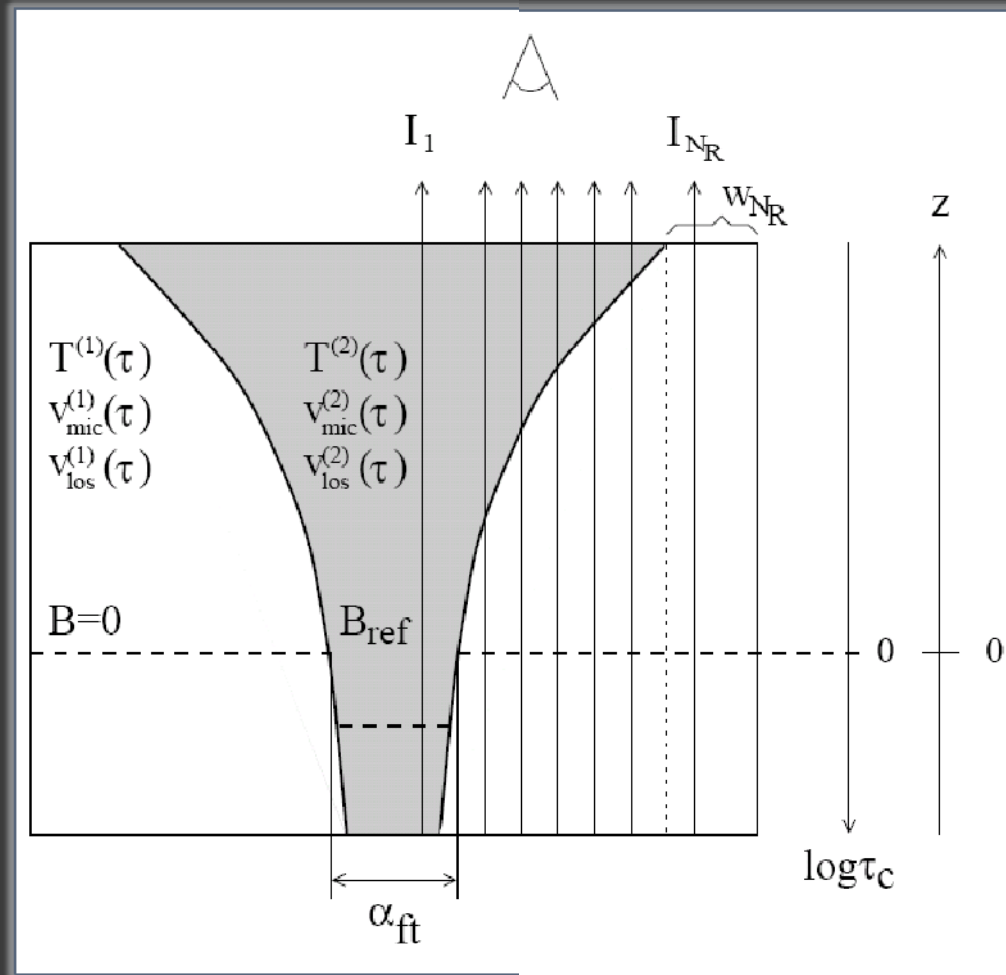


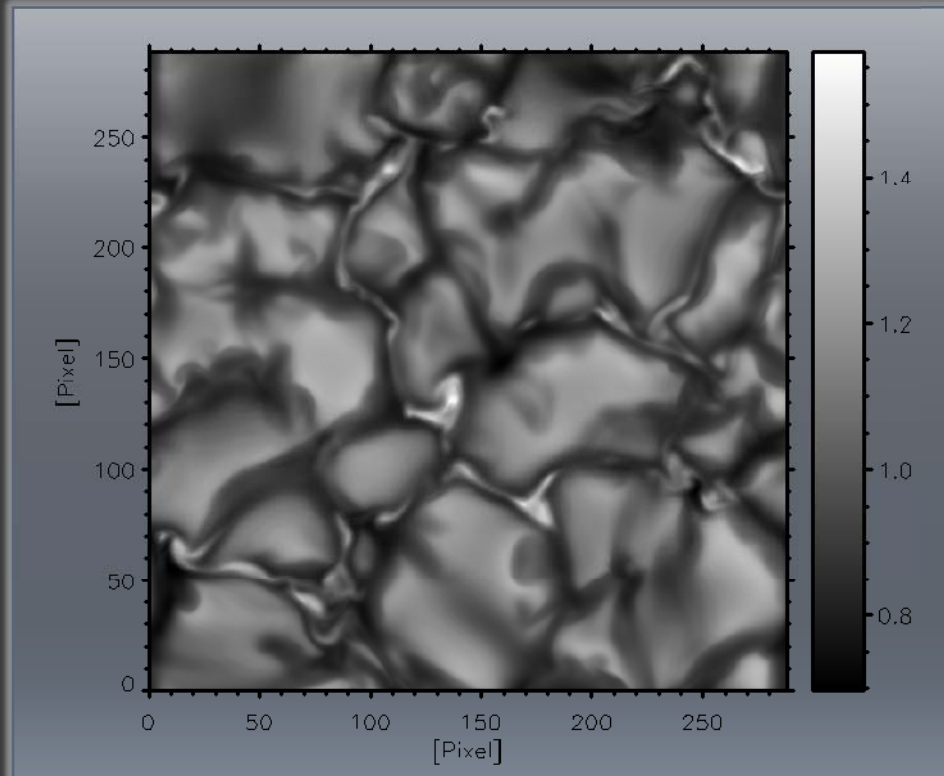
# SPINOR

## Inversions based on RFs



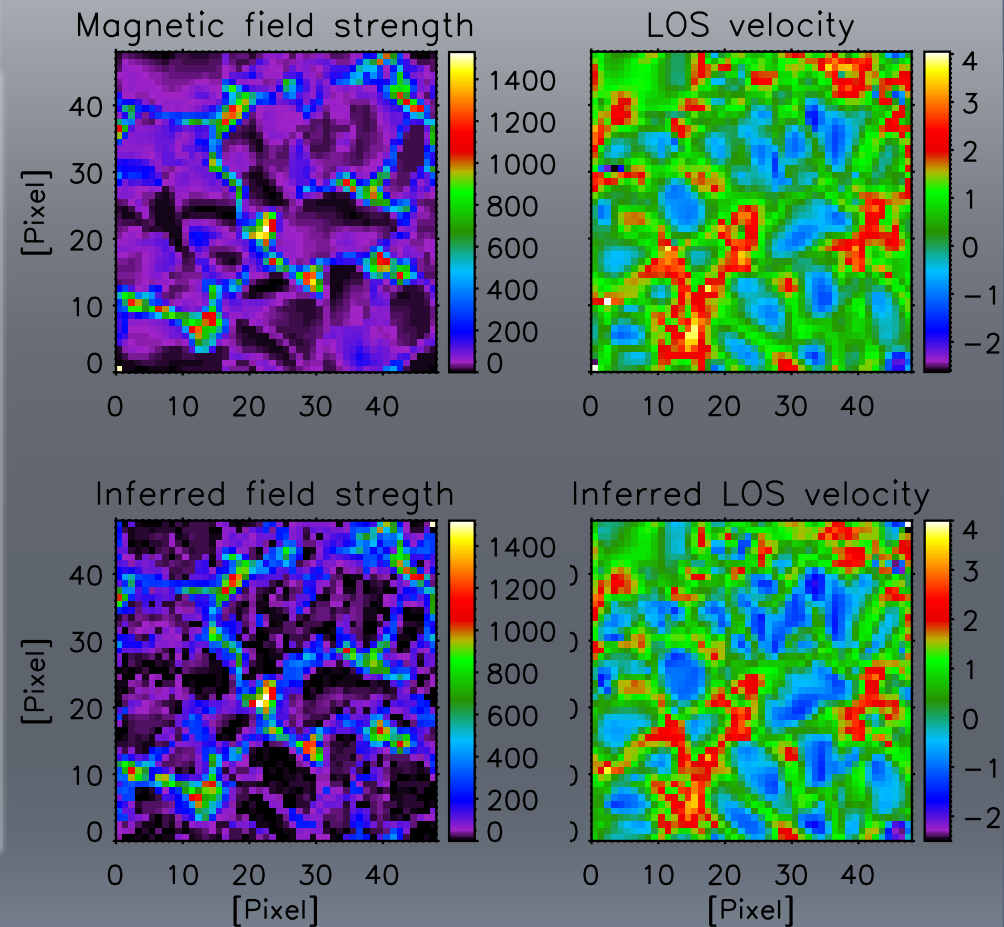
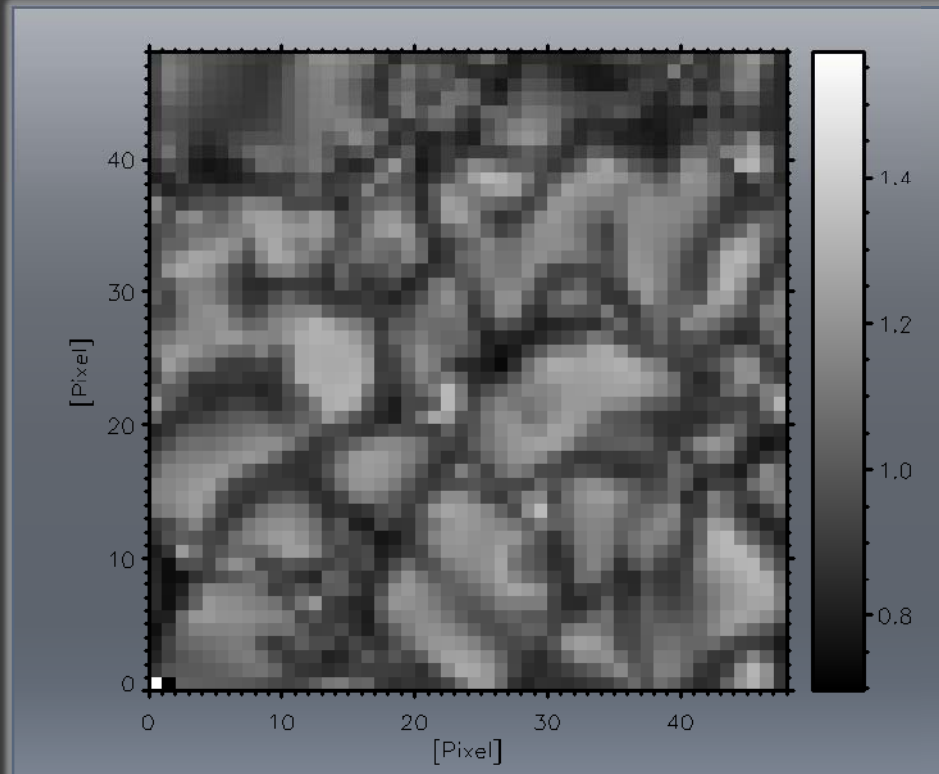
# Asymmetric profiles and ME (1)

MHD-Simulations (Vögler et al. 2005)



# Asymmetric profiles and ME (2)

## MHD-Simulations (Vögler et al. 2005)

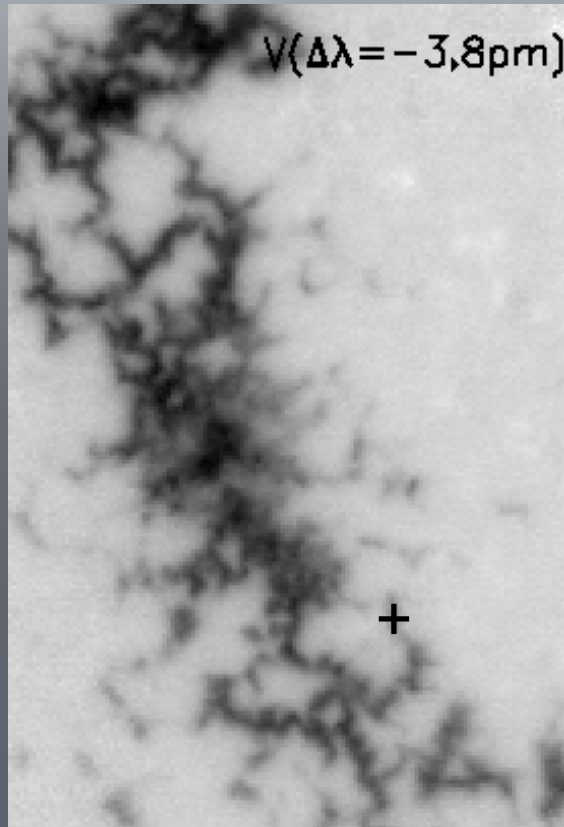


➤ Fe I 630.1 and 630.2 profiles degraded to SP pixel size

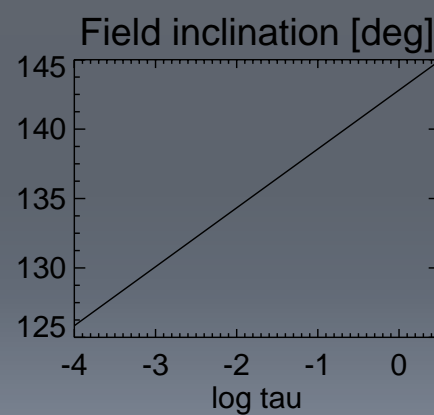
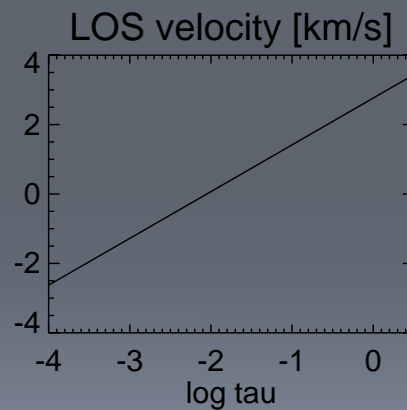
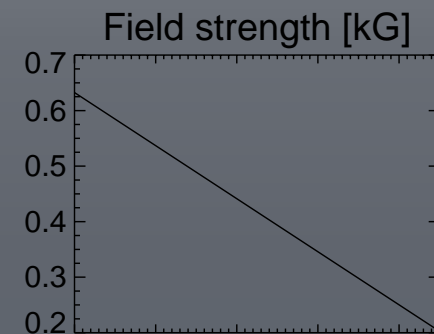
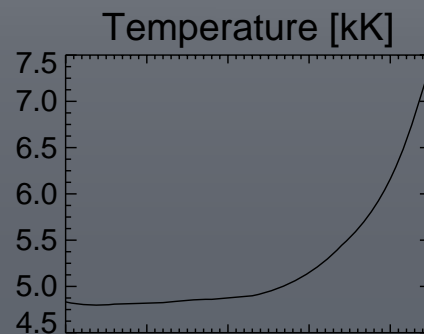
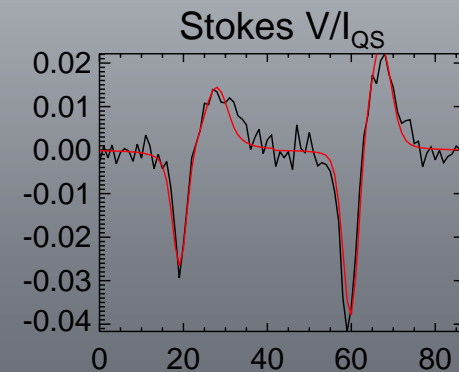
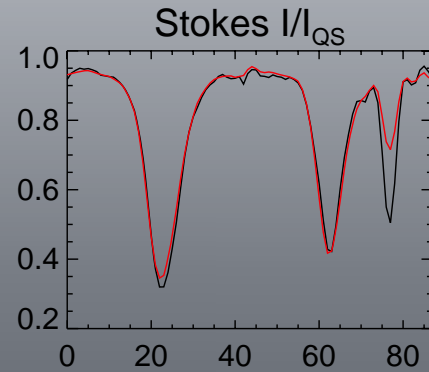
➤ Maps of inferred  $B$  and  $v_{\text{LOS}}$  very similar to real ones!

# Inversions with gradients

- Inversion codes capable of dealing with gradients
  - Are based on numerical solution of RTE
  - Provide reliable thermal information
  - Use *less free parameters than ME codes (7 vs 8)*
  - Infer stratifications of physical parameters with depth
  - Produce better fits to asymmetric Stokes profiles
- Height dependence of atmospheric parameters is needed for
  - easier solution of the  $180^\circ$  azimuth disambiguity
  - 3D structure of sunspots and pores
  - Magnetic flux cancellation events
  - Polarity inversion lines
  - Dynamical state of coronal loop footpoints
  - wave propagation analysis
  - ...



- Spatial resolution:  $\sim 0.4''$
- VIP + TESOS + KAOS
- Inversion: SIR with 10 free parameters



# Non-ME Inversion Codes

<b>SIR</b>	Ruiz Cobo & del Toro Iniesta (1992)	1C & 2C atmospheres, arbitrary stratifications, any photospheric line
<b>SIR/FT</b>	Bellot Rubio et al. (1996)	Thin flux tube model, arbitrary stratifications, any photospheric line
<b>SIR/NLTE</b>	Socas-Navarro et al. (1998)	NLTE line transfer, arbitrary stratifications
<b>SIR/GAUS</b>	Bellot Rubio (2003)	Uncombed penumbral model, arbitrary stratifications
<b>SPINOR</b>	Frutiger & Solanki (2001)	1C & 2C (nC) atmospheres, arbitrary stratifications, any photospheric line, molecular lines, flux tube model, uncombed model
<b>LILIA</b>	Socas-Navarro (2001)	1C atmospheres, arbitrary stratifications
<b>MISMA IC</b>	Sánchez Almeida (1997)	MISMA model, arbitrary stratifications, any photospheric line

# SPINOR core: the synthesis

- RTE has to be solved for
  - each spectral line
  - each line-of sight
  - each iteration
- efficient computation required!

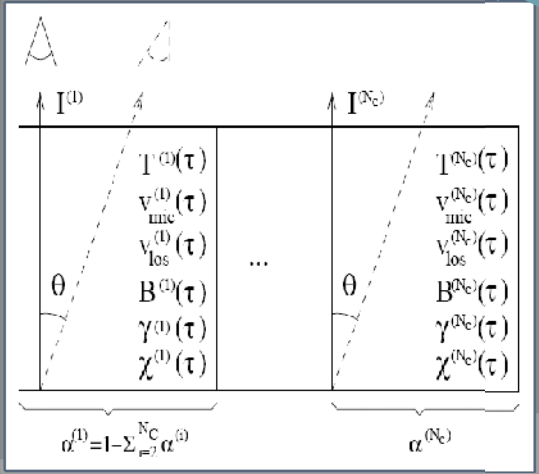
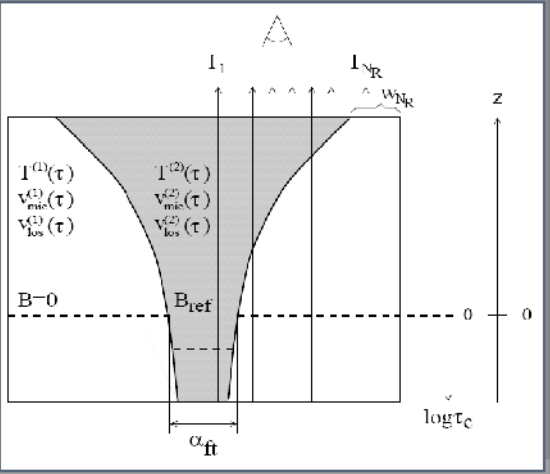
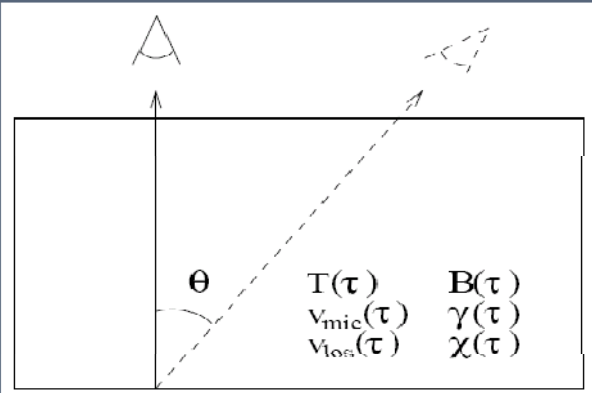
atmospheric parameters:

- T ... gas temperature
- B ... magn. field strength
- $\gamma, \phi$  ... incl. / azimuth angle of B
- $v_{LOS}$  ... line-of sight velocity
- $v_{mic}$  ... micro-turbulent velocity

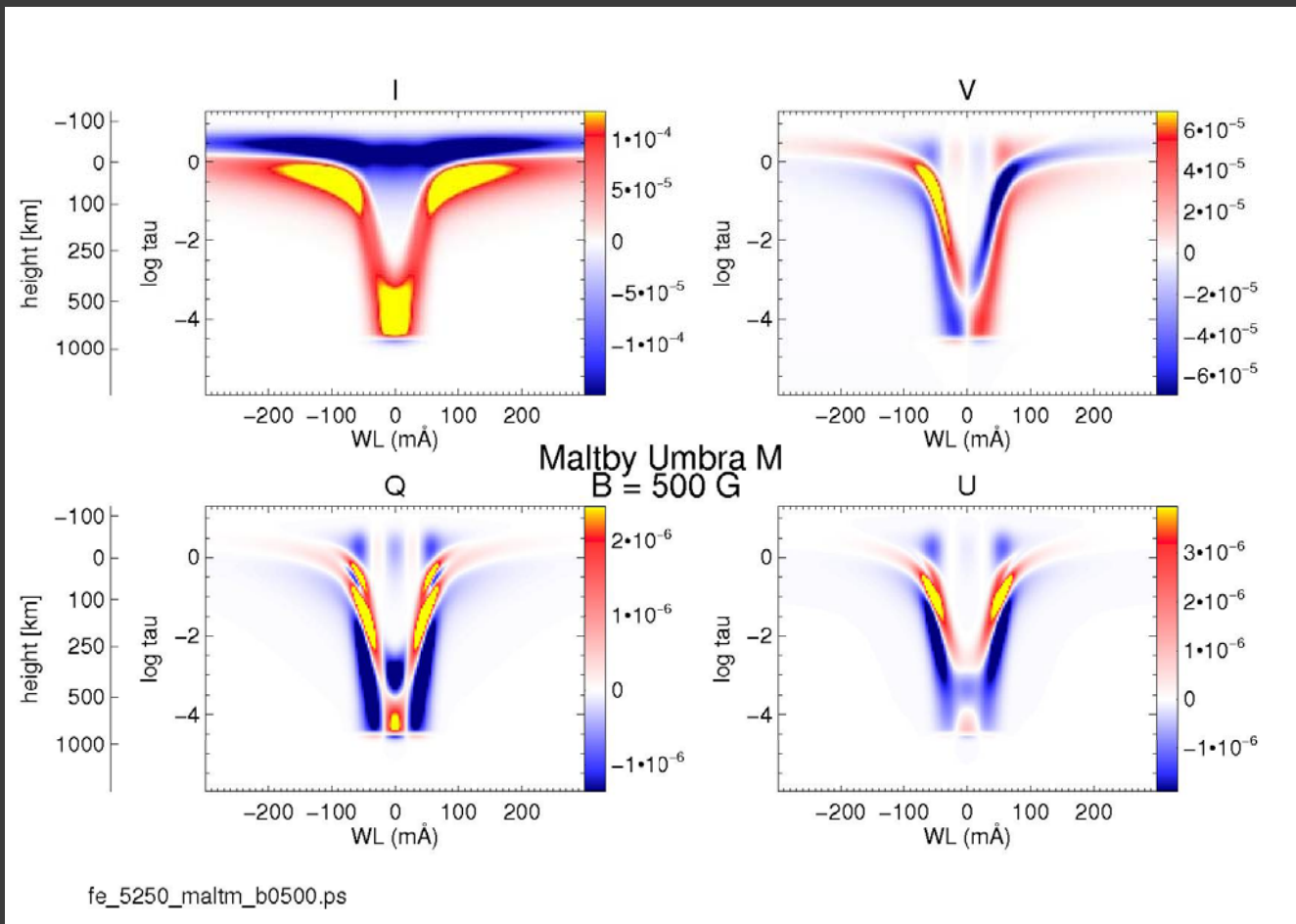
- $A_X$  ... abundance ( $A_H=12$ )
- G ... grav. acc. at surface
- $v_{mac}$  ... macro-turbulence
- $v_{inst}$  ... instr. broadening
- $v_{abs}$  ... abs. velocity Sun-Earth

height / tau dependent

height independent



# Stokes sepctrum diagnostics CFs and RFs





# Contribution Functions (1)

The contribution function (CF) describes how different atmospheric layers contribute to the observed spectrum.

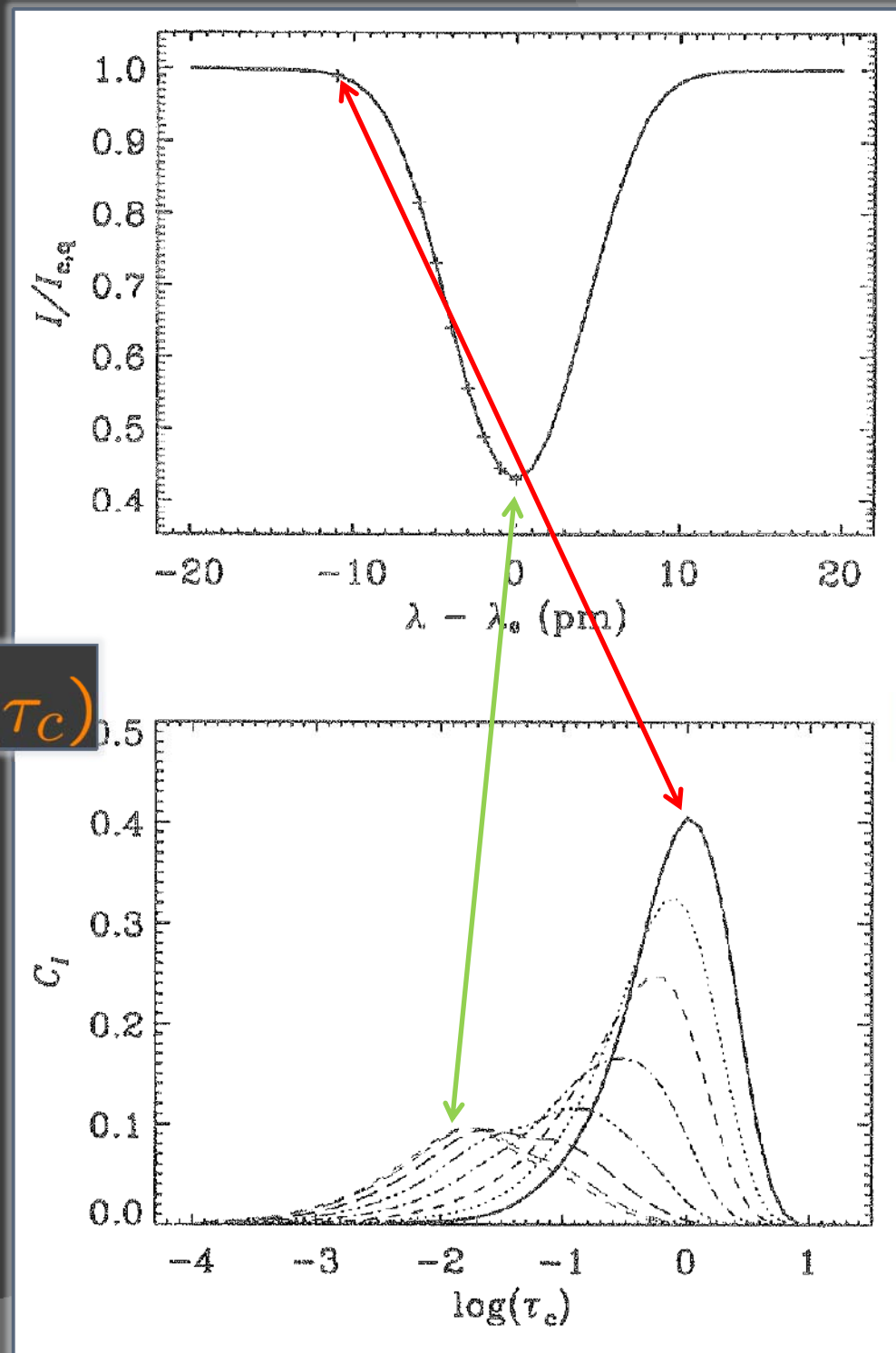
Mathematical definition:

CF  $\equiv$  integrand of formal sol. of RTE (here isotropic case, no B field):

$$C(\tau_c) \equiv e^{-\int_0^\infty k(t) dt} k(\tau_c) S(\tau_c)$$

line core: highest formation  
wings: lowest formation

Intuitively: profile shape indicates atmospheric opacity. Medium is more transparent (less heavily absorbed) in wings.  $\rightarrow$  one can see „deeper“ into the atmosphere at the wings.



# Contribution functions (2)

The general case:

$$\mathbf{C}(\tau_c) \equiv \mathbf{O}(0, \tau_c) \mathbf{K}(\tau_c) \mathbf{S}(\tau_c)$$

Height of formation:

„This line is formed at x km above the reference, the other line is formed at y km ...“

→ caution with this statement is highly recommended!

→ CFs are strongly dependent on model atmosphere

→ different physical quantities are measured at different atmospheric heights

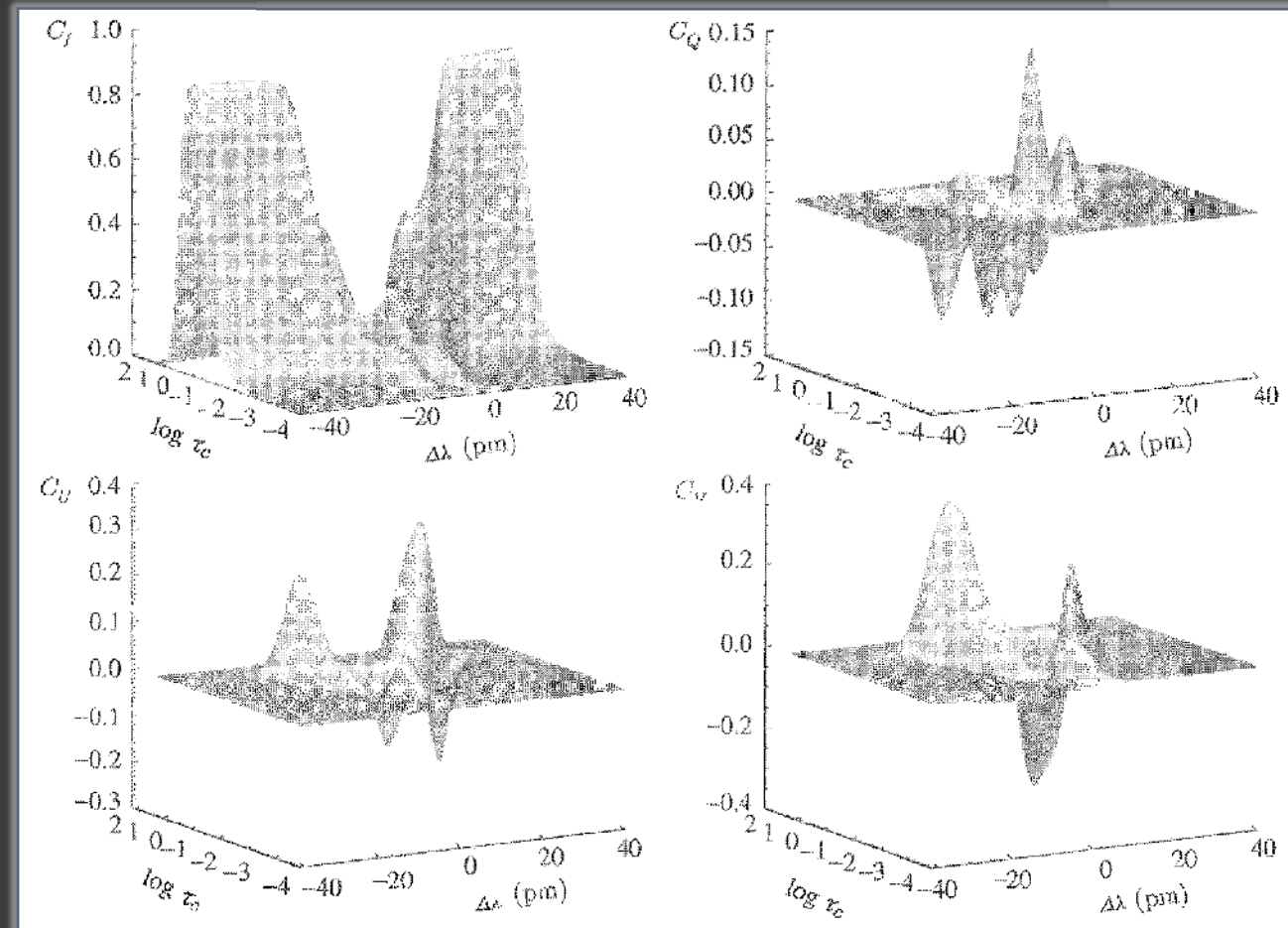
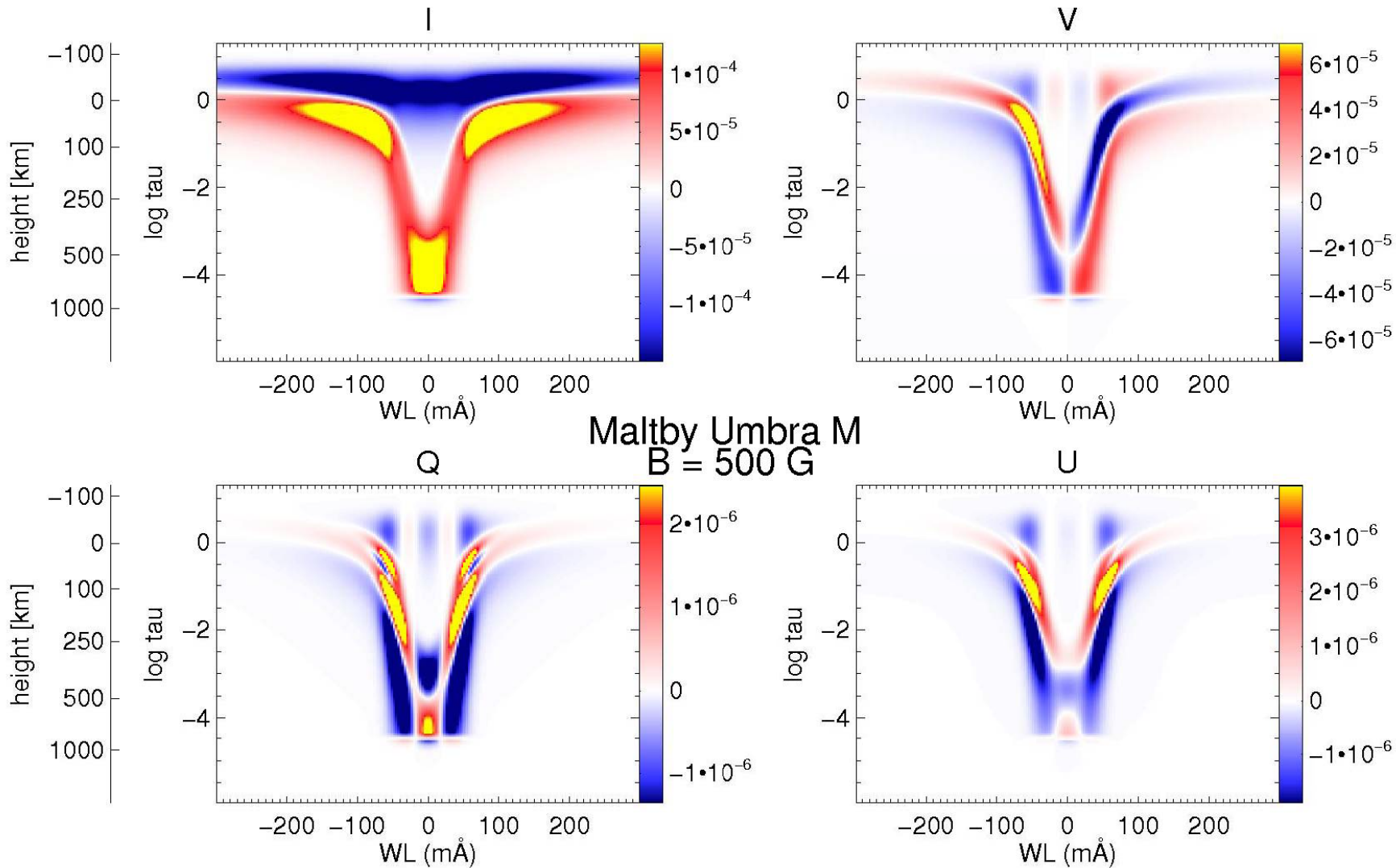


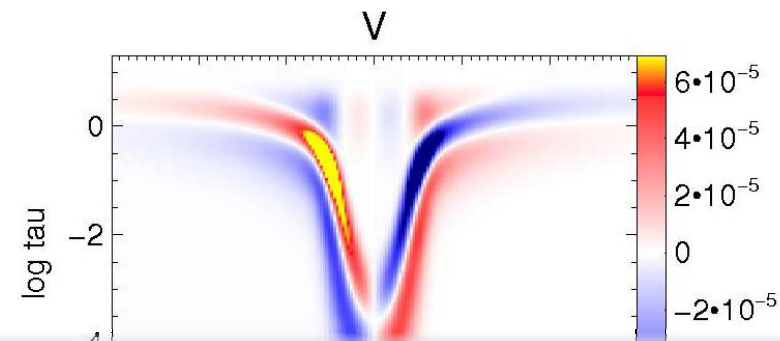
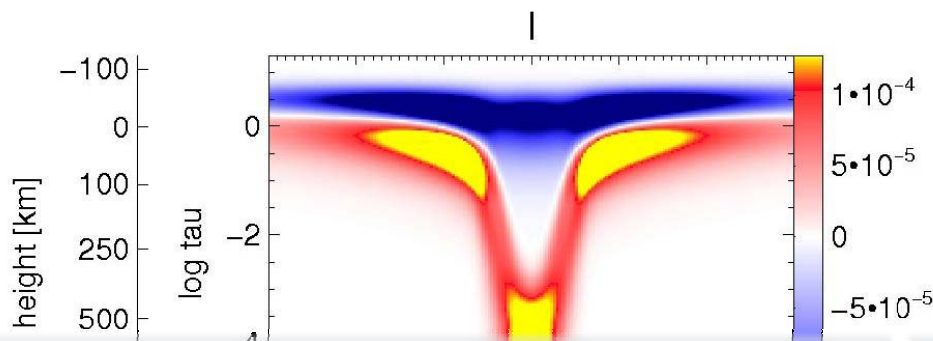
Fig. 10.6. Contribution function of the Fe I line at 630.25 nm in the penumbral model of Fig. 9.3. Wavelength is along the Y axis and logarithmic optical depth along the X axis.

# Response Functions



fe\_5250\_maltm\_b0500.ps

# Response Functions



## „brute force method“:

1. synthesis of Stokes spectrum in given model atmosphere
2. perturbation of one atm. parameter
3. synthesis of „perturbed“ Stokes spectrum
4. calculation of ratio between both spectra
5. repeat (2)-(4) for all  $\tau_i$ ,  $\lambda_i$ , atm. parameter, atm. comp.

## The smart way:

- knowledge of source function, evolution operator and propagation matrix
- direct computation of RFs possible (all parameters known from solution of RTE, simple derivatives)

WL (mÅ)

# Response functions

Linearization: small perturbation in physical parameters of the model atmosphere propagate „linearly“ to small changes in the observed Stokes spectrum.

$$\delta\mathbf{K}(\tau_c) = \sum_{i=1}^m \frac{\partial\mathbf{K}}{\partial x_i} \delta x_i(\tau_c), \quad \delta\mathbf{S}(\tau_c) = \sum_{i=1}^m \frac{\partial\mathbf{S}}{\partial x_i} \delta x_i(\tau_c)$$

introduce these modifications into RTE:

$$\frac{d(\mathbf{I} + \delta\mathbf{I})}{d\tau_c} = (\mathbf{K} + \delta\mathbf{K})(\mathbf{I} + \delta\mathbf{I} - \mathbf{S} - \delta\mathbf{S})$$

only take 1<sup>st</sup> order terms, and introduce  $\tilde{\mathbf{S}} = \delta\mathbf{S} - \mathbf{K}^{-1}\delta\mathbf{K}(\mathbf{I} - \mathbf{S})$

$$\tilde{\mathbf{C}}(\tau_c) \equiv \mathbf{O}(0, \tau_c) \mathbf{K}(\tau_c) \tilde{\mathbf{S}}(\tau_c) \equiv \sum_{i=1}^m \mathbf{R}_i(\tau_c) \delta x_i(\tau_c)$$

contribution function to perturbations of observed Stokes profiles

response functions

## Response Functions (2)

RFs have the role of **partial derivatives** of the Stokes profiles **with respect to the physical quantities** of the model atmosphere:

$$\delta \mathbf{I}(0) = \sum_{i=1}^m \int_0^{\infty} \mathbf{R}_i(\tau_c) \delta x_i(\tau_c) d\tau_c$$

In words:

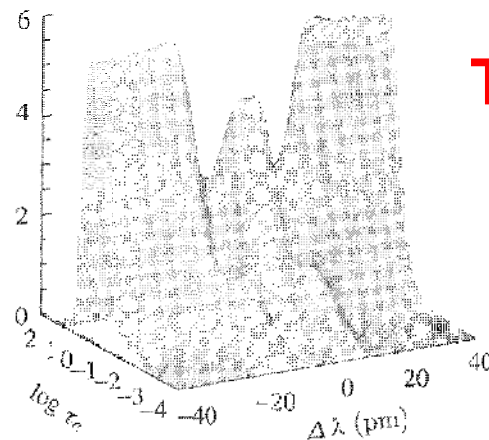
If  $x_k$  is modified by a unit perturbation in a restricted neighborhood around  $\tau_0$ , then the values of  $R_k$  around  $\tau_0$  give us the ensuing variation of the Stokes vector.

Response function units are inverse of their corresponding quantities (e.g RFs to temperature have units  $K^{-1}$ )

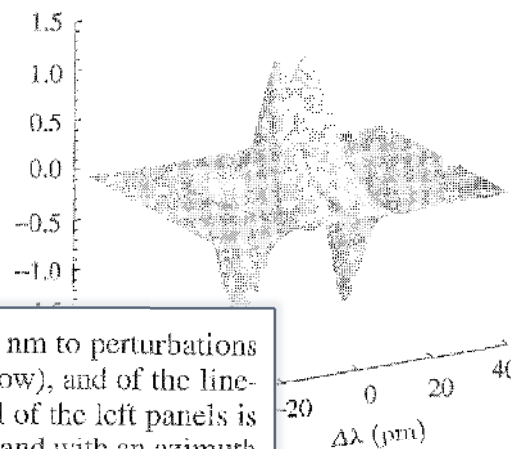
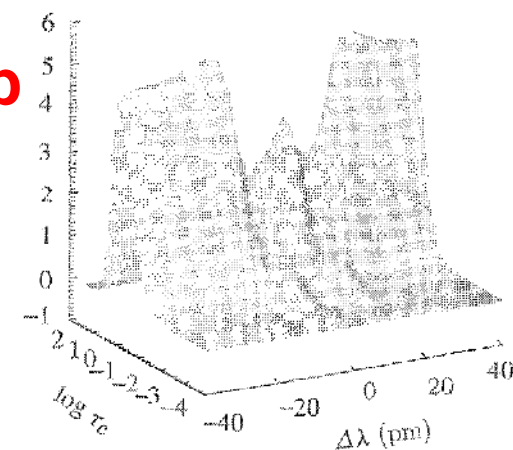
# RFs – Example: Fe 6302.5

model on the left is:

- 500 K hotter
- 500 G stronger
- 20° more inclined
- 50° larger azimuth
- no VLOS gradient (right: linear gradient)



Temp



|B|

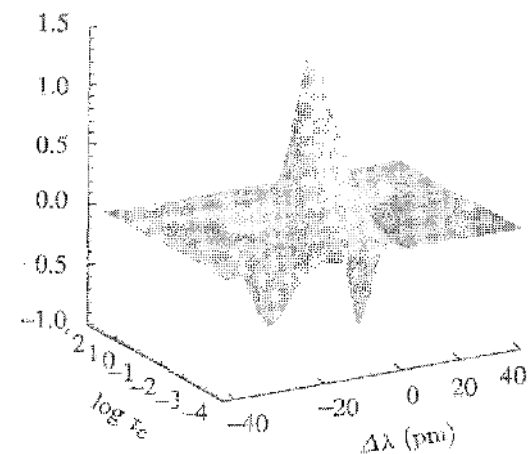
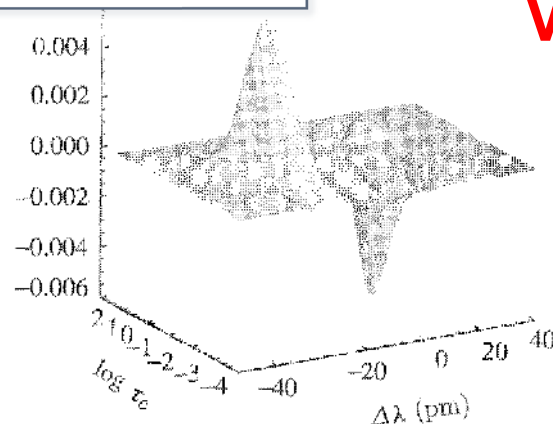
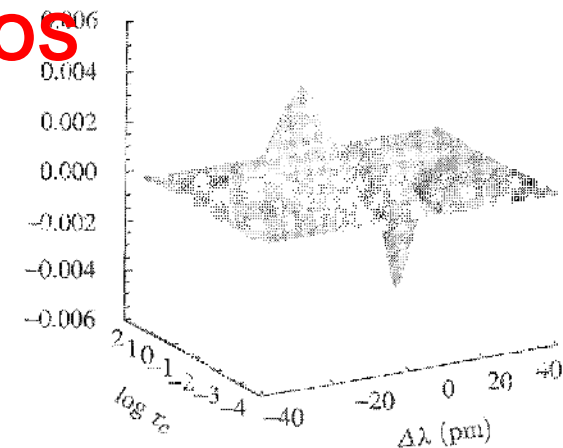


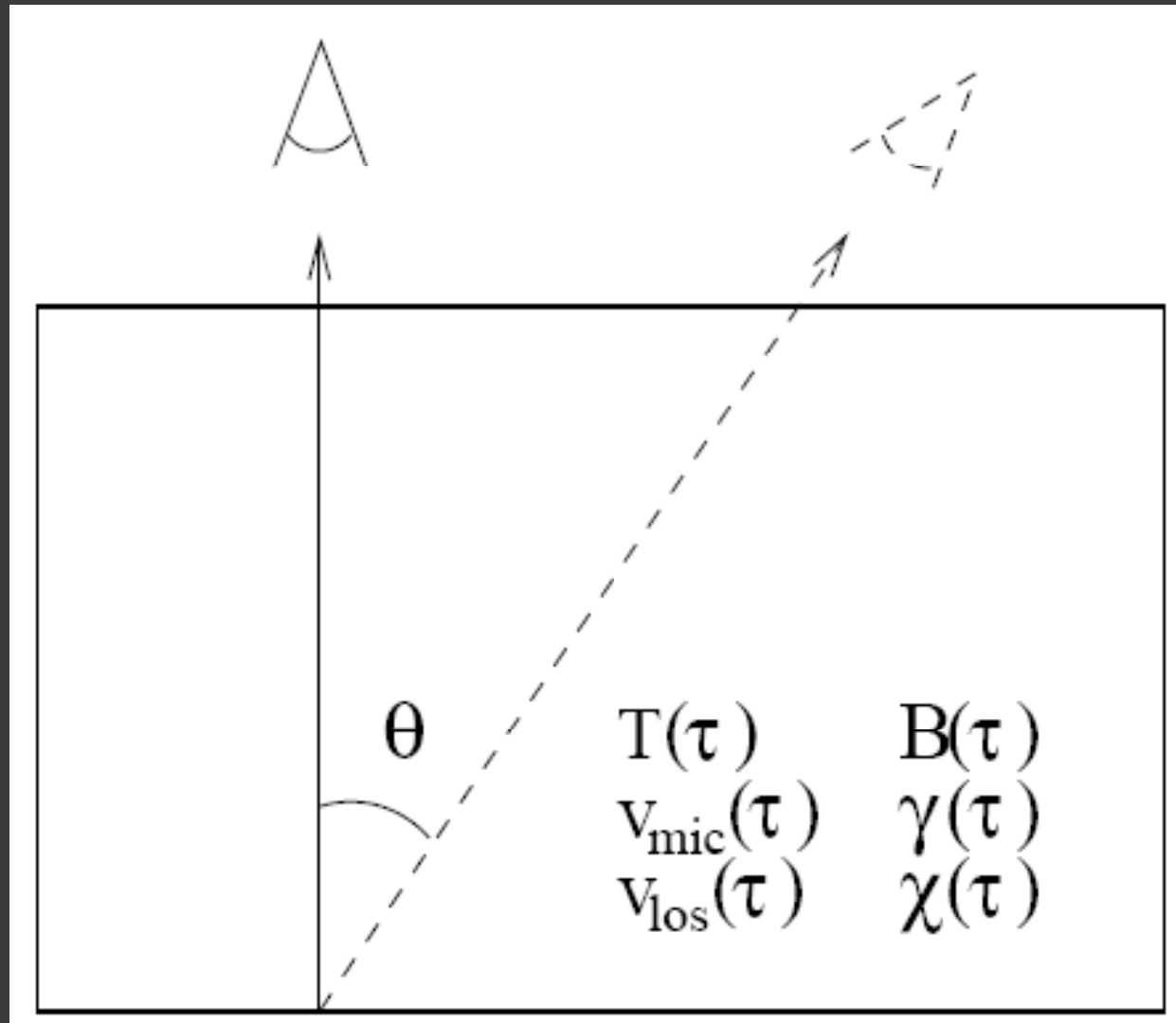
Fig. 10.8. Response functions of Stokes  $I$  of the Fe I line at 630.25 nm to perturbations of the temperature (top row), of the magnetic field strength (middle row), and of the line-of-sight velocity (bottom row) in two model atmospheres. The model of the left panels is 500 K hotter, has a magnetic field 500 G stronger, 20° more inclined, and with an azimuth 50° larger than the model of the right panels. The latter has a linear gradient of the LOS velocity whereas the former is at rest. Wavelength is along the Y axis (in pm with respect to the center of the line) and logarithmic optical depth along the X axis.



VLOS

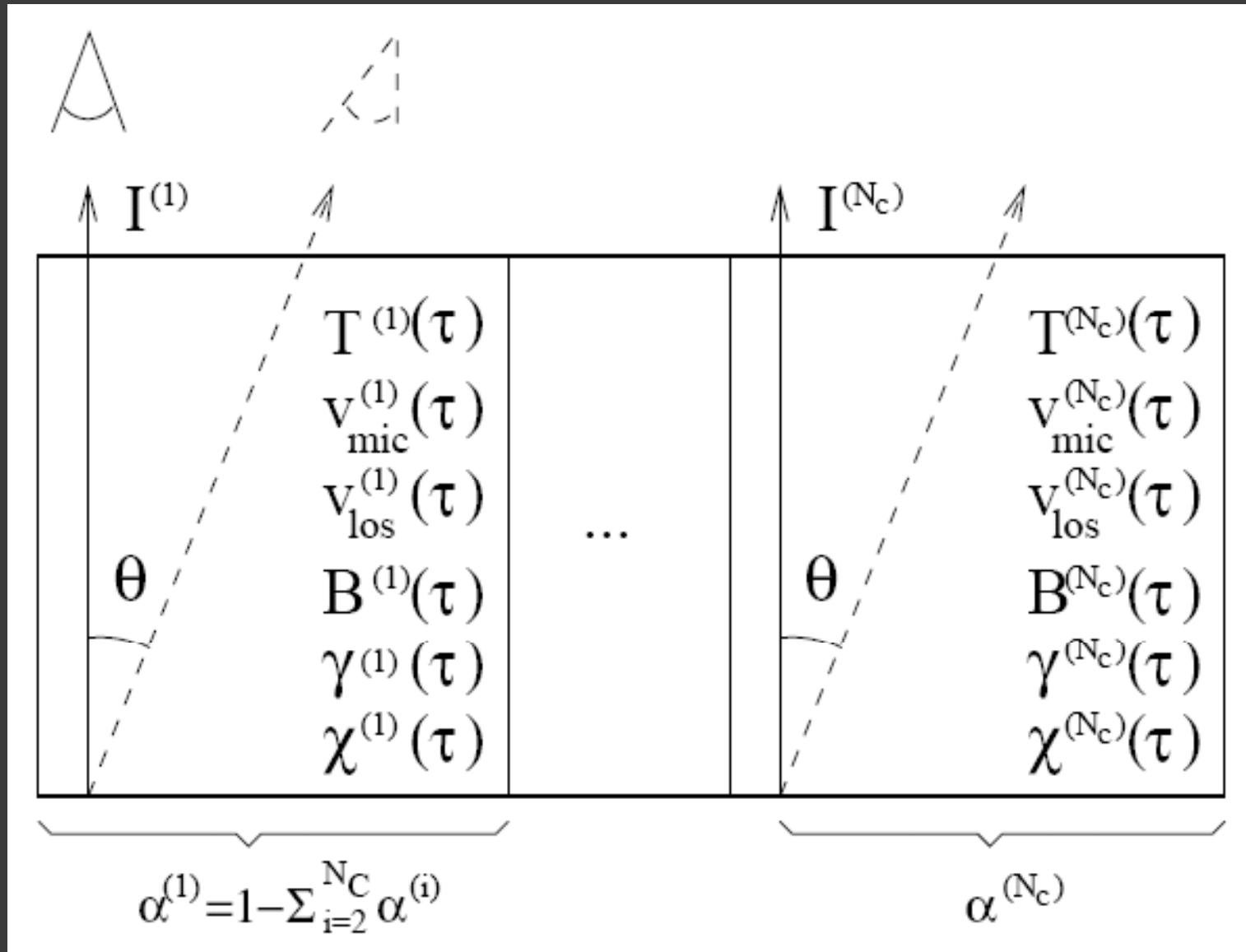


# SPINOR: complex model atmospheres

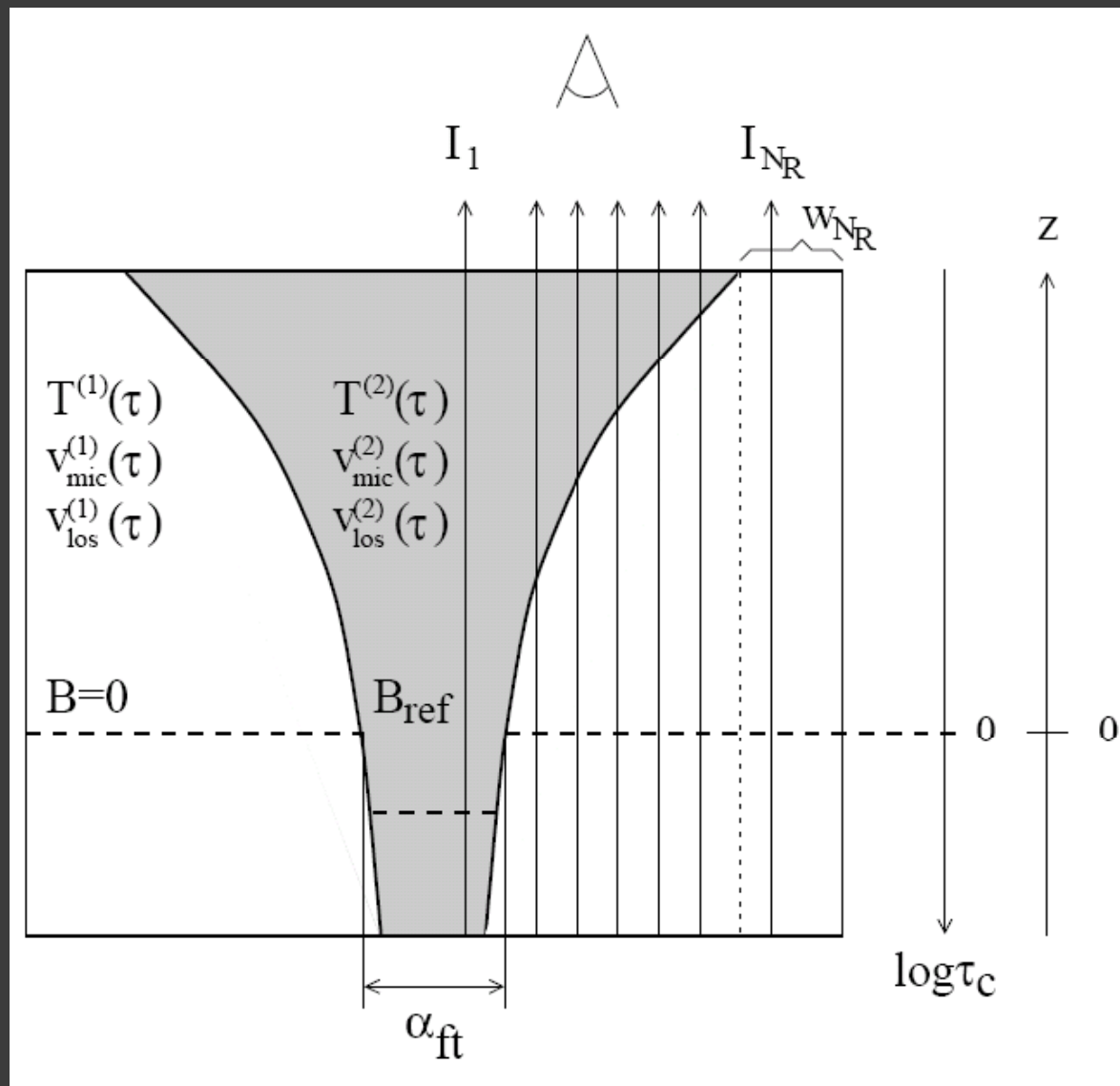




# The even more complex case:



# The fluxtube case:



# The complex fluxtube case:

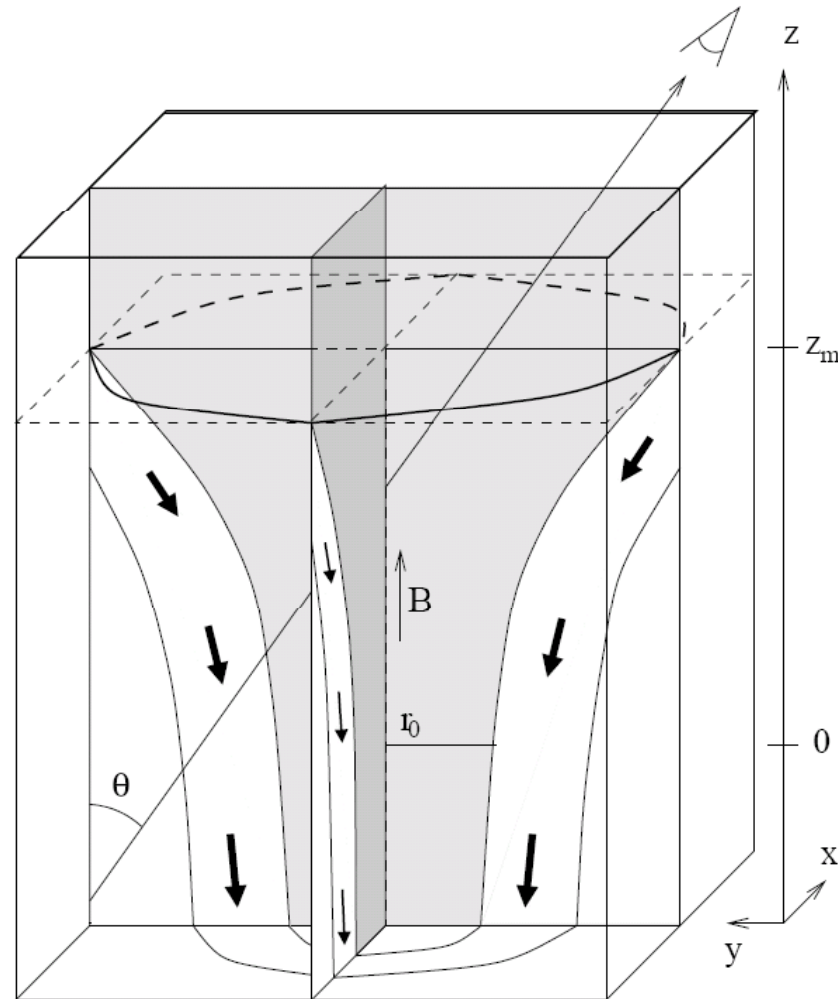
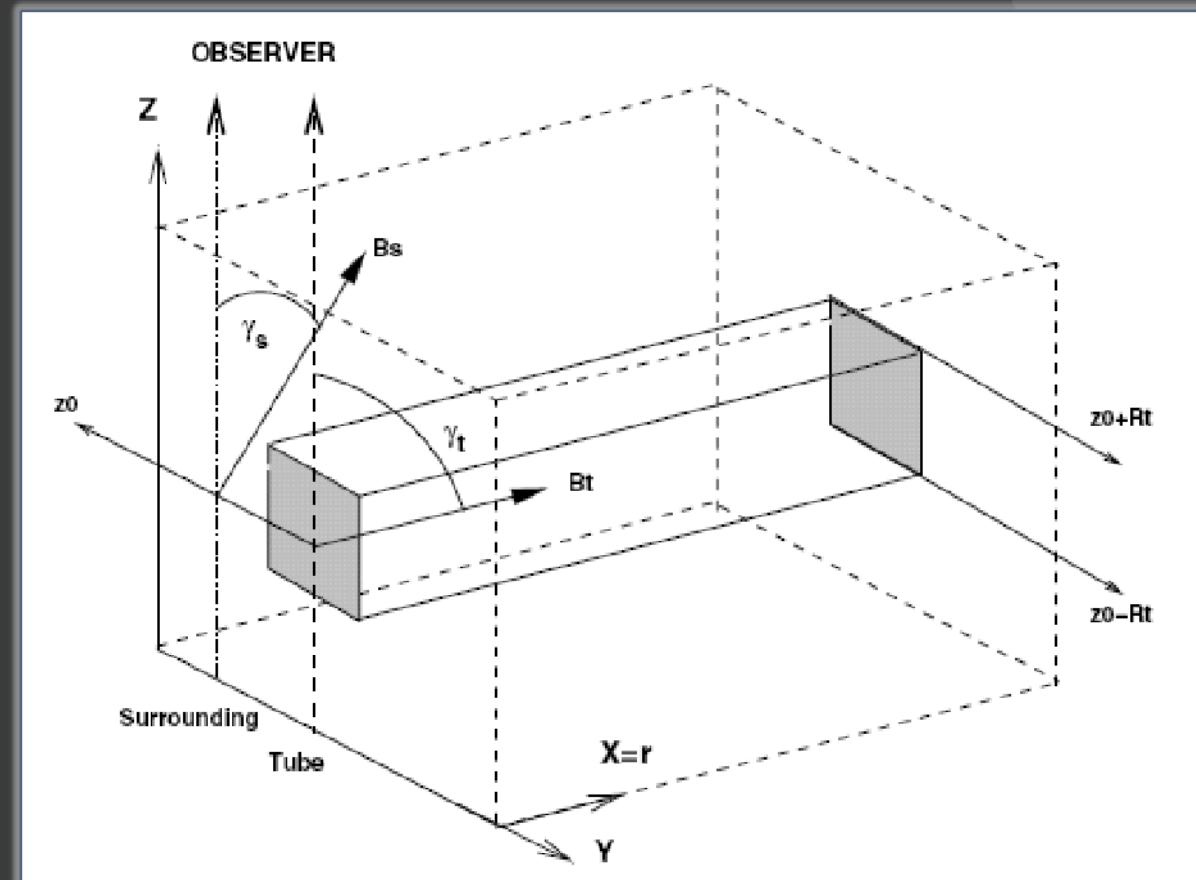


**Figure 7.4:** Vertical cuts through schematic flux-tube cell. The shaded area represents the flux-tube interior filled with a magnetic field. The non-magnetic surroundings are expected to harbor strong downflows (thick arrows) along the tube boundaries. Net velocities as seen by the observer, i.e. Doppler shifts entering the radiative transfer equations, are obtained by projection on the lines of sights (thin arrows). For position away from disk center ( $\mu = \cos\theta < 1$ ), the flux tube thus must be treated as a quasi 3-dimensional structure.

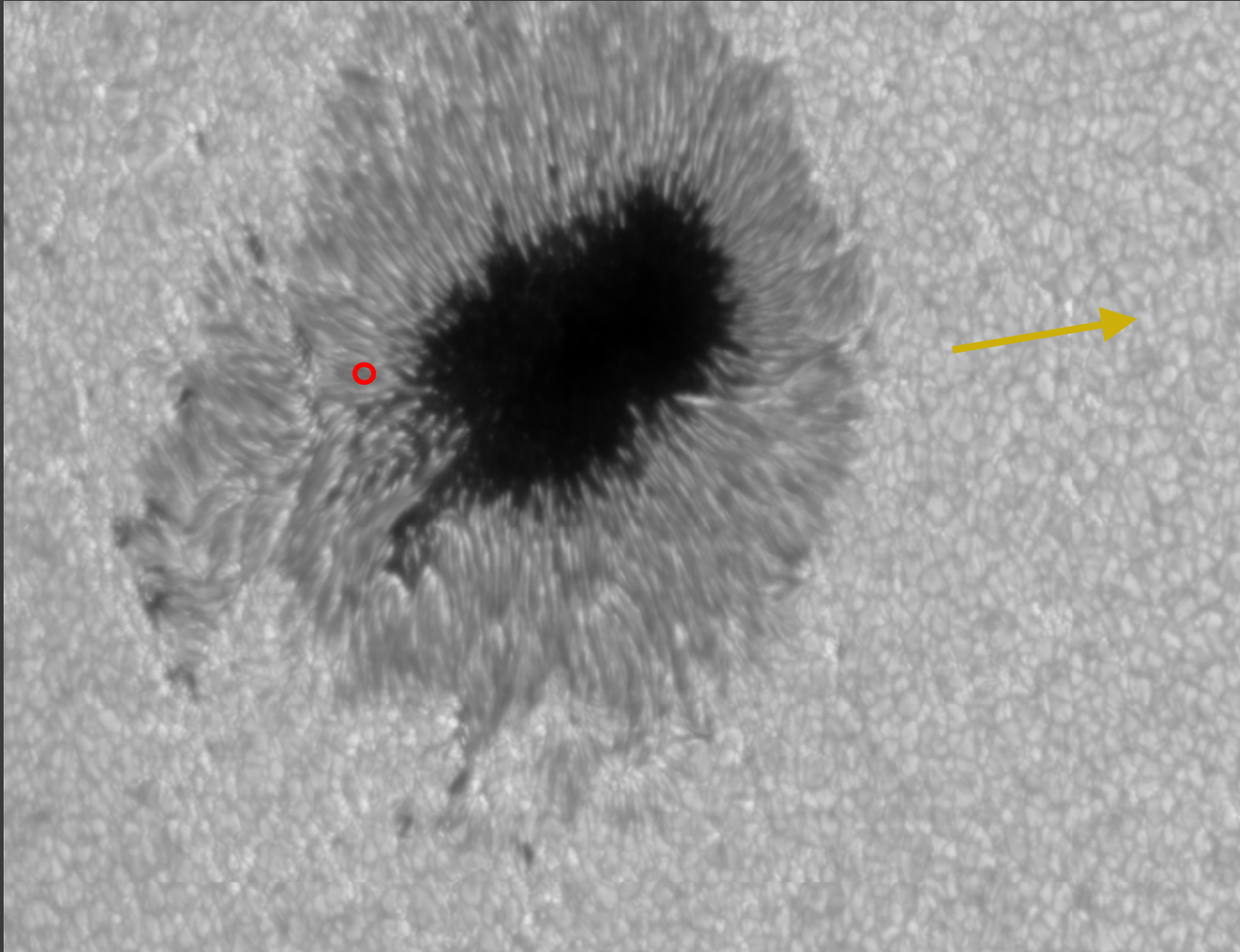
# SPINOR: Versatility

- Plane-parallel, **1-component models** to obtain averaged properties of the atmosphere
- **Multiple components** (e.g. to take care of scattered light, or unresolved features on the Sun). Allows for arbitrary number of magnetic or field-free components (turns out to be important, e.g. in flare observations, where we have seen 4-5 components).
- **Flux-tubes** in total pressure equilibrium with surroundings, at arbitrary inclination
  - in field-free (or weak-field surroundings)
  - embedded in strong fields (e.g. sunspot penumbra, or umbral dots)
  - includes the presence of multiple flux tubes along a ray when computing away from disk centre
  - efficient computation of lines across jumps in atmospheric quantities
- **Integration over solar or stellar disk**, including solar/stellar rotation
- **molecular lines** (S. Berdyugina)
- non-LTE (MULTI 2.2, **not tested** yet, requires brave MULTI expert)

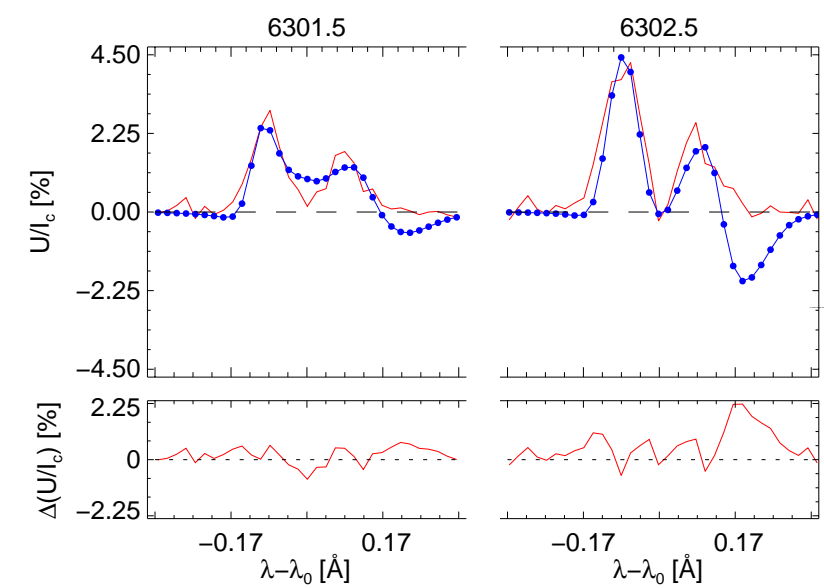
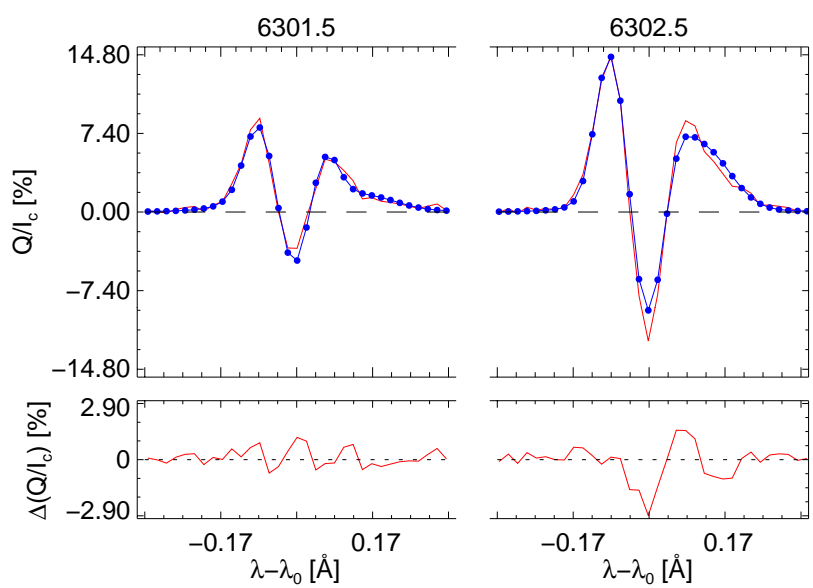
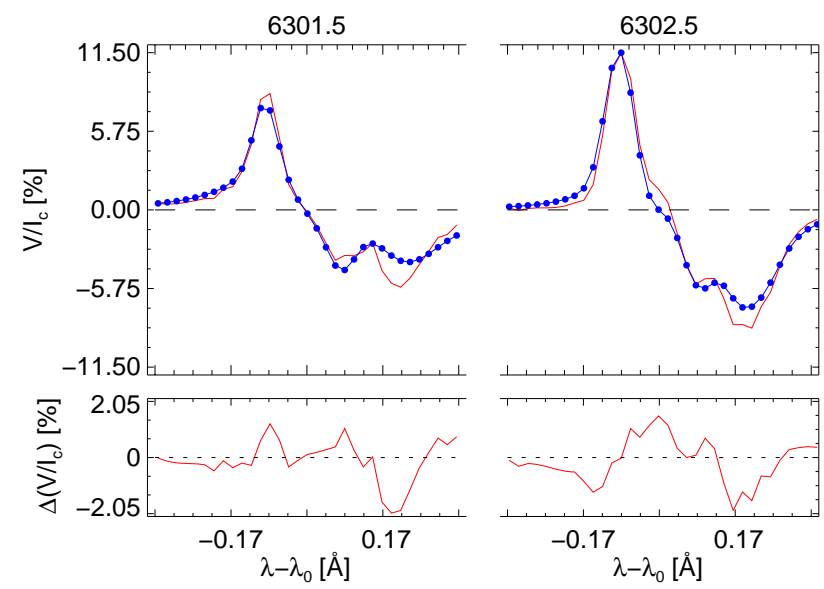
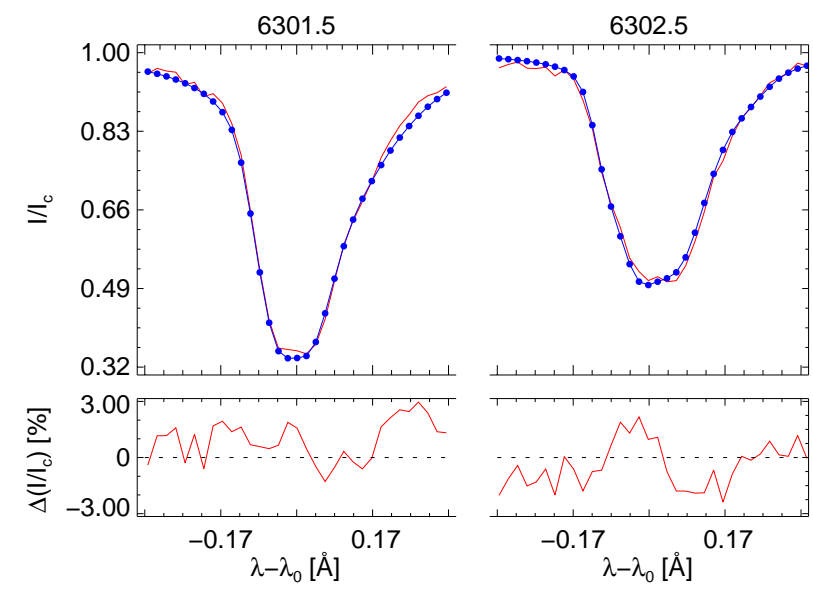
- SPINOR applied to:  
Fe I 6301 + 6302  
Fe I 6303.5  
Ti I 6303.75
- 1st component:  
tube ray (discontinuity  
at boundary)
- 2nd component:  
surrounding ray



Hinode SOT: 10-11-2006



inv\_070214.051204\_hinode\_test.tgz

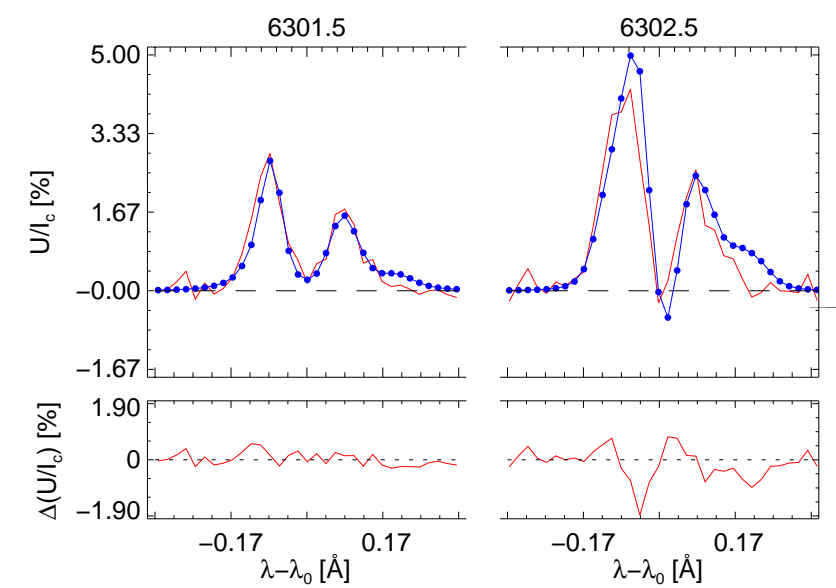
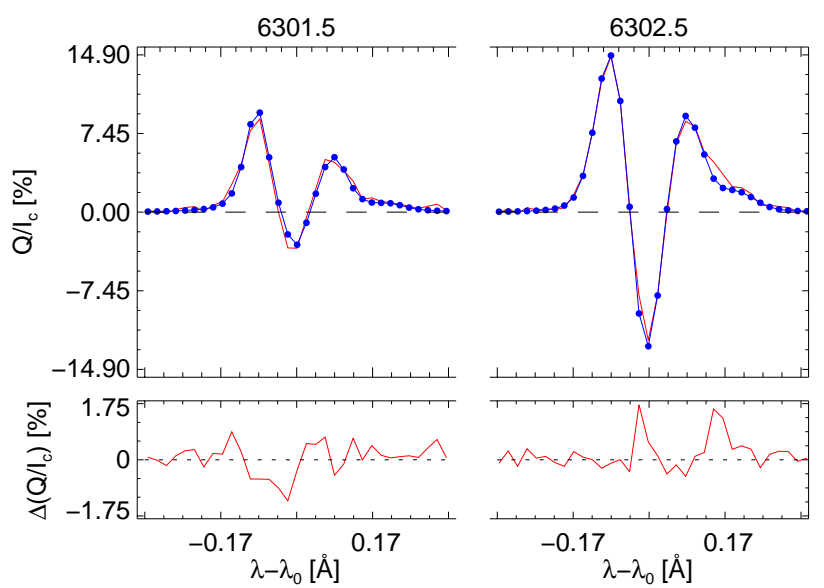
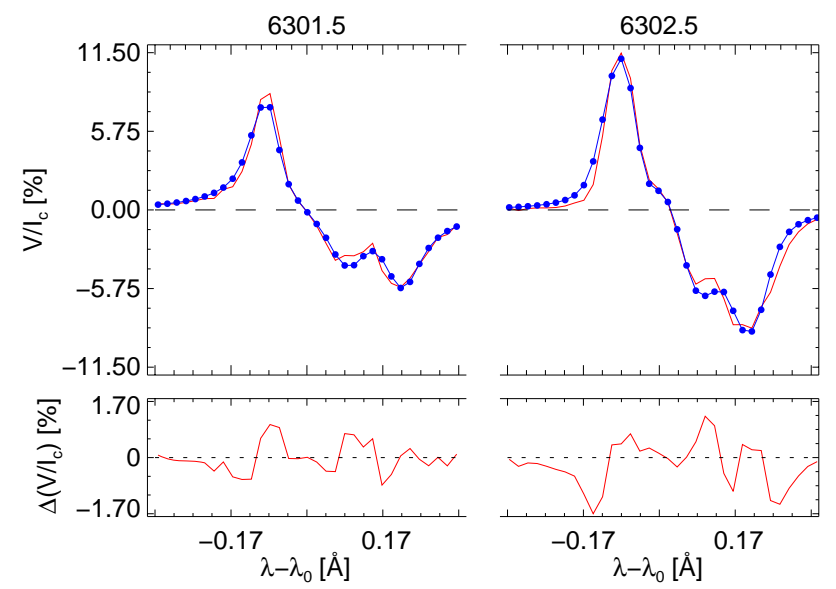
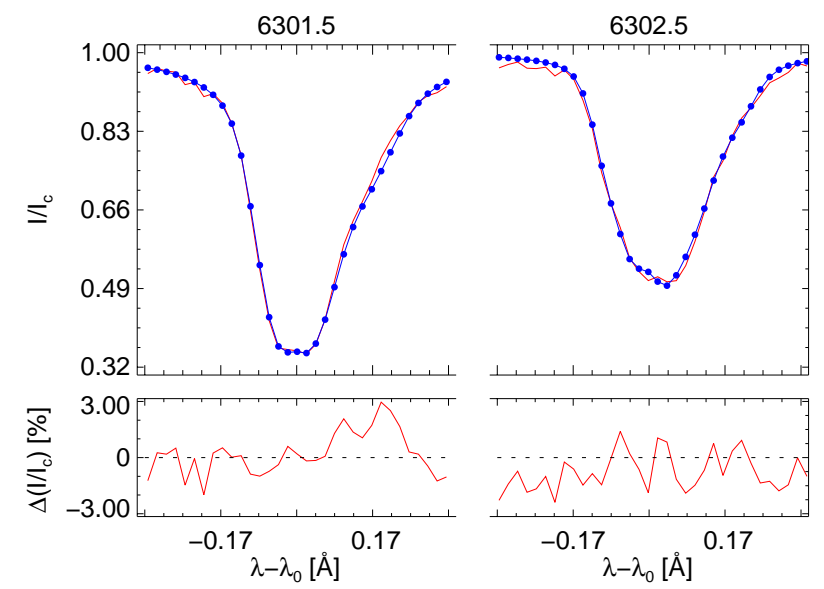


FINAL ATM IC= 1 WL= 5000.0000

FINAL ATM IC= 1 WL= 5000.0000

FINAL ATM IC= 1 WL= 5000.0000

inv\_070214.024925\_hinode\_test.tgz



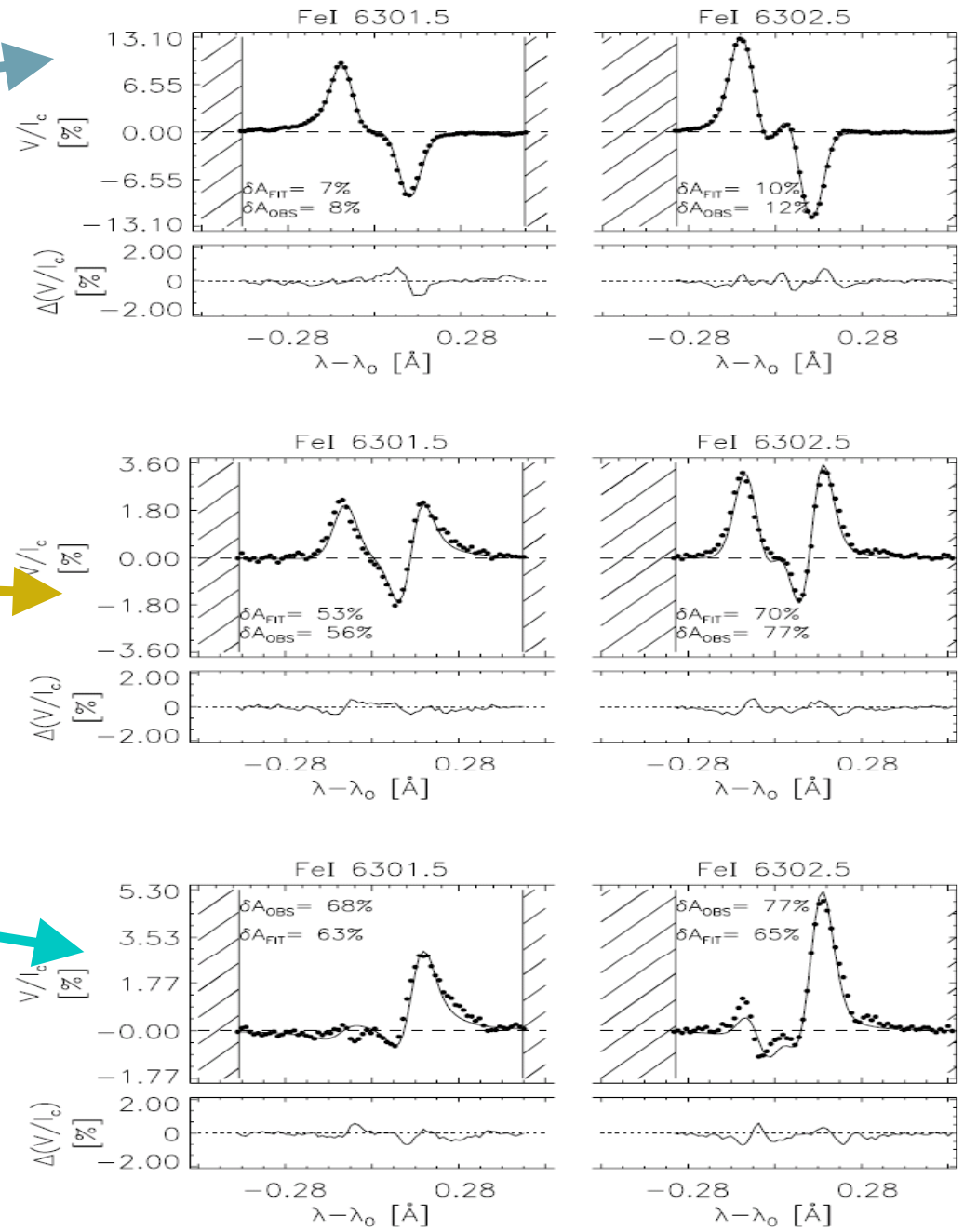
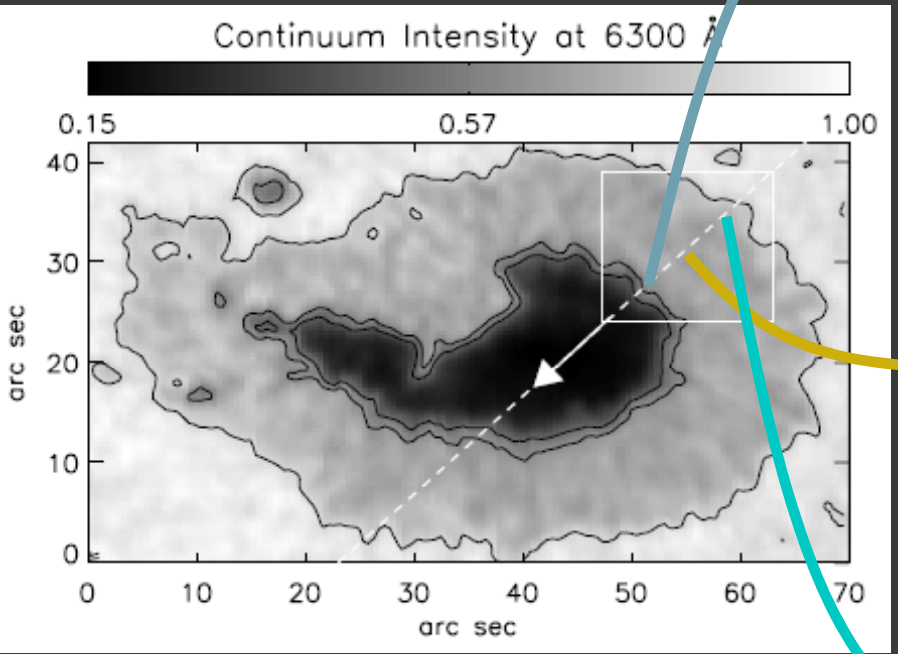
FINAL ATM IC= 2 WL= 5000.0000

FINAL ATM IC= 2 WL= 5000.0000

FINAL ATM IC= 2 WL= 5000.0000

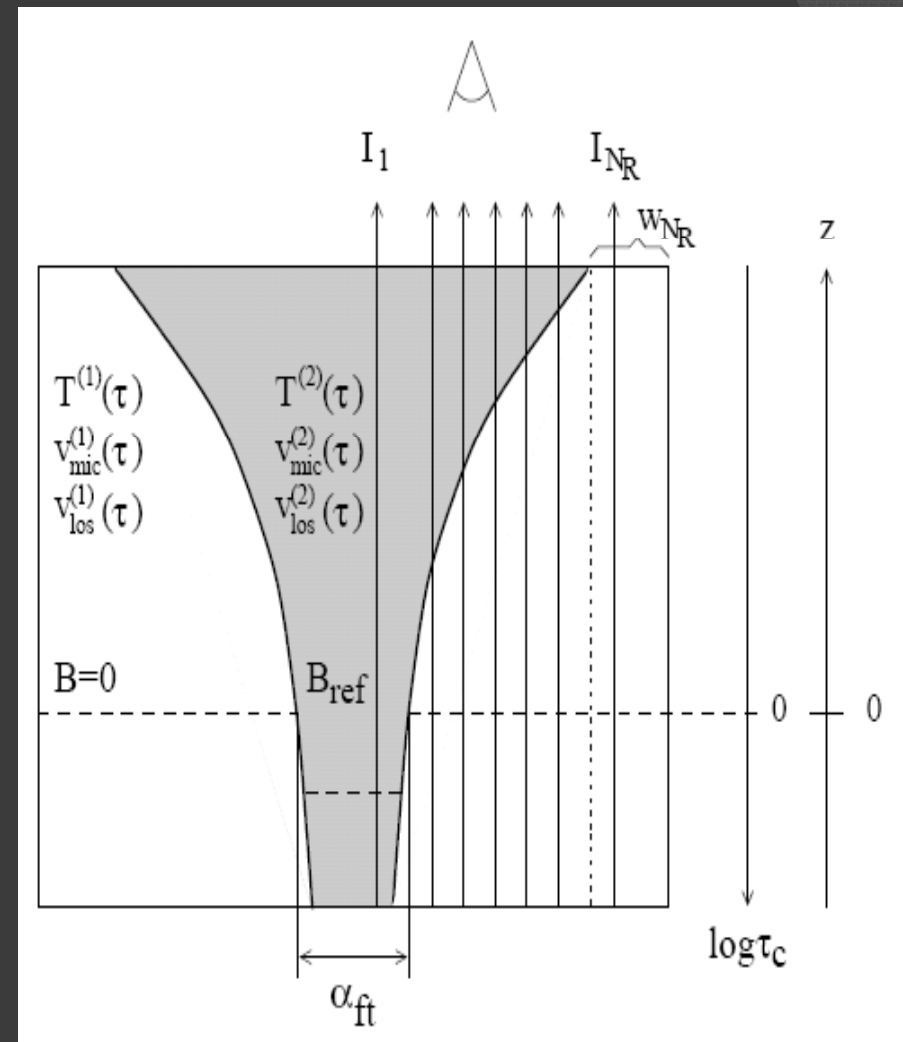
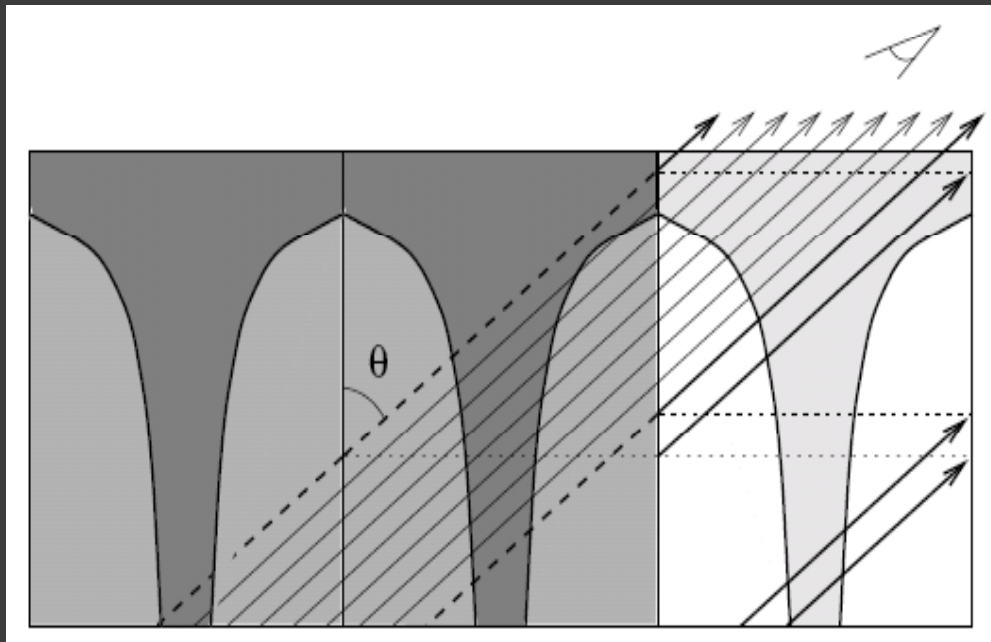






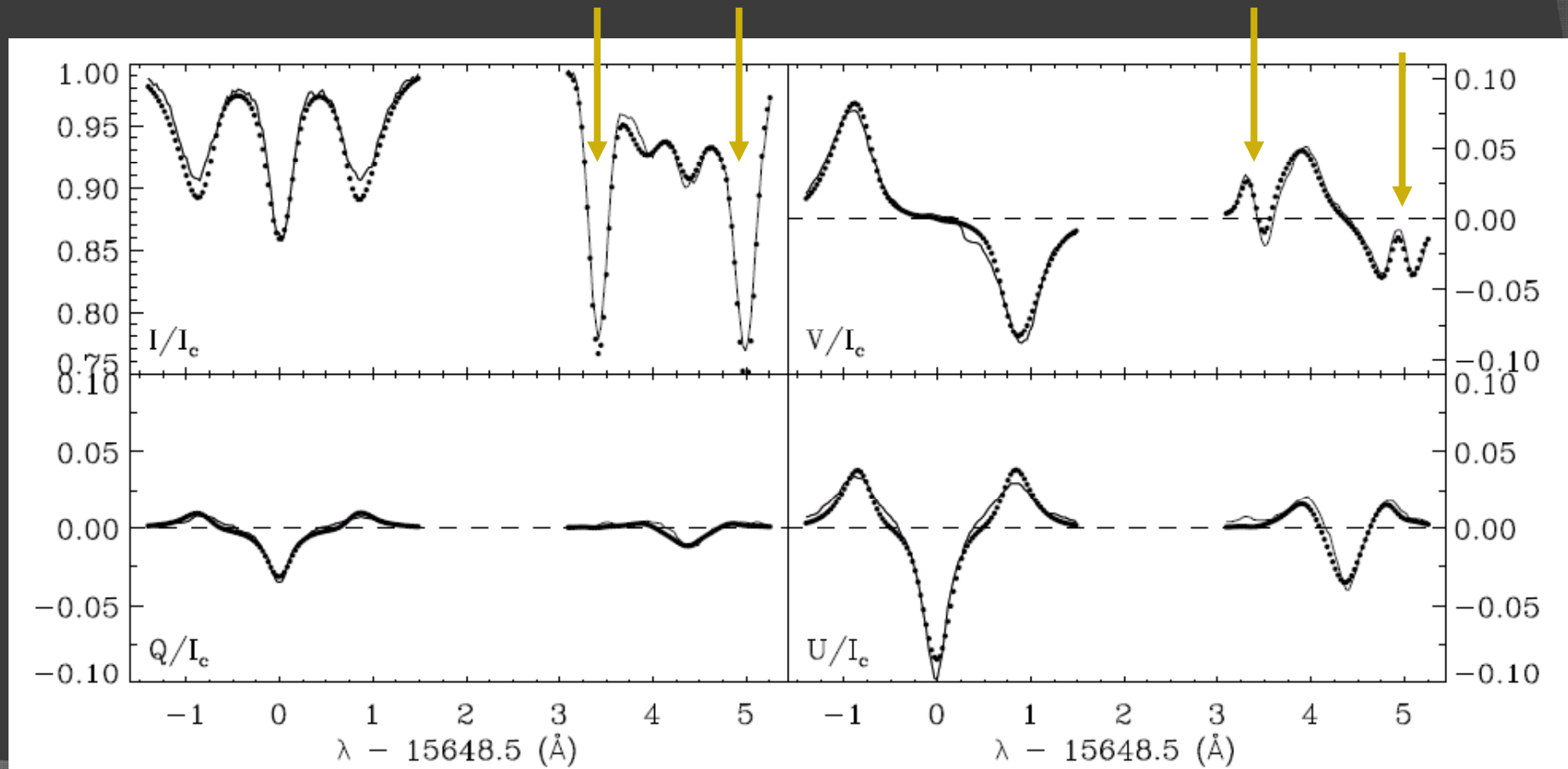
→ confirms uncombed model  
 → flux tube thickness 100-300 km

- multiple rays
- pressure balance
- broadening of flux tube

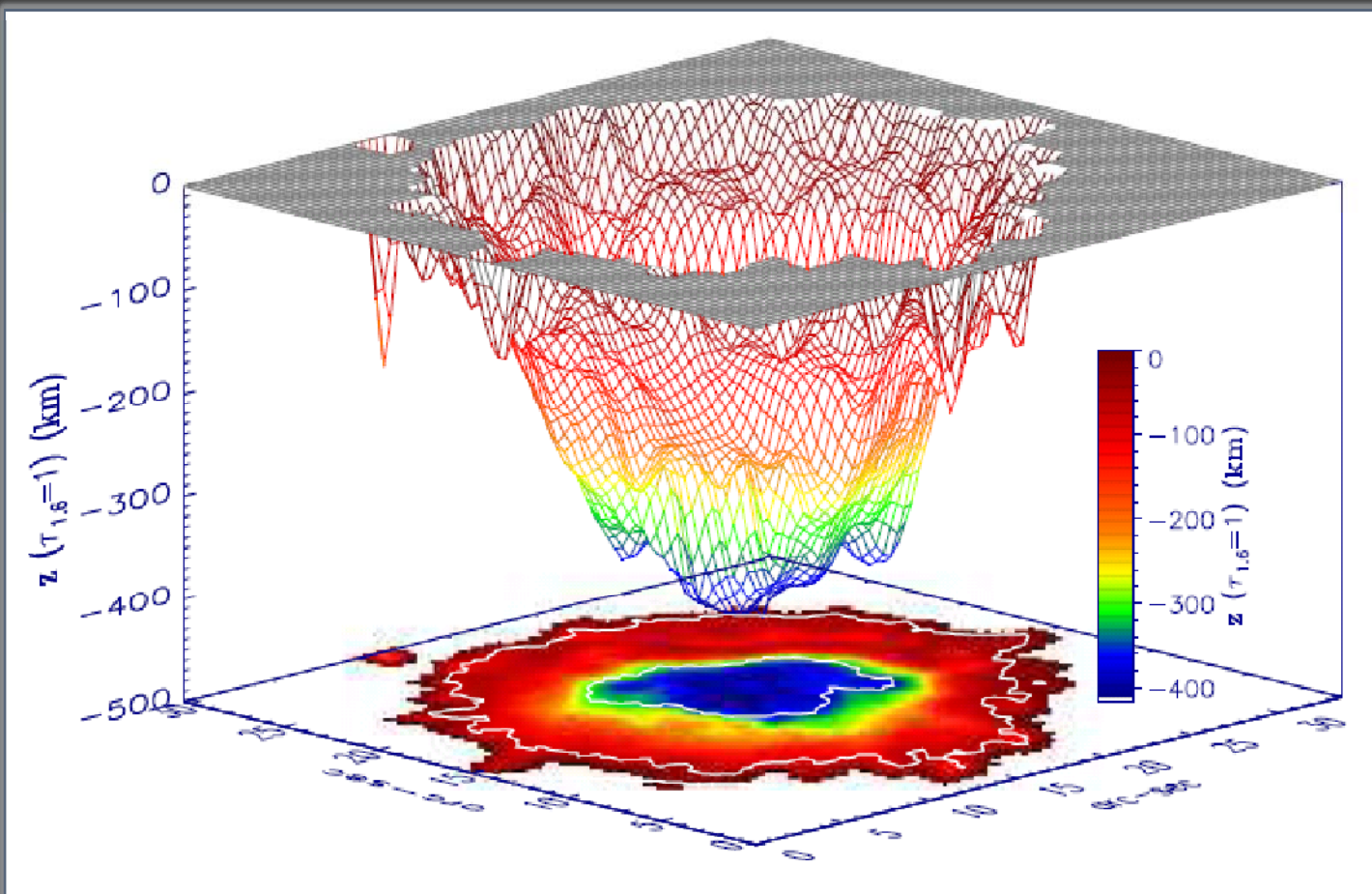


- SPINOR applied to:  
Fe I 15648 / 15652
- 1 magn. comp (6 nodes)  
1 straylight comp.
- molecular OH lines

with OH

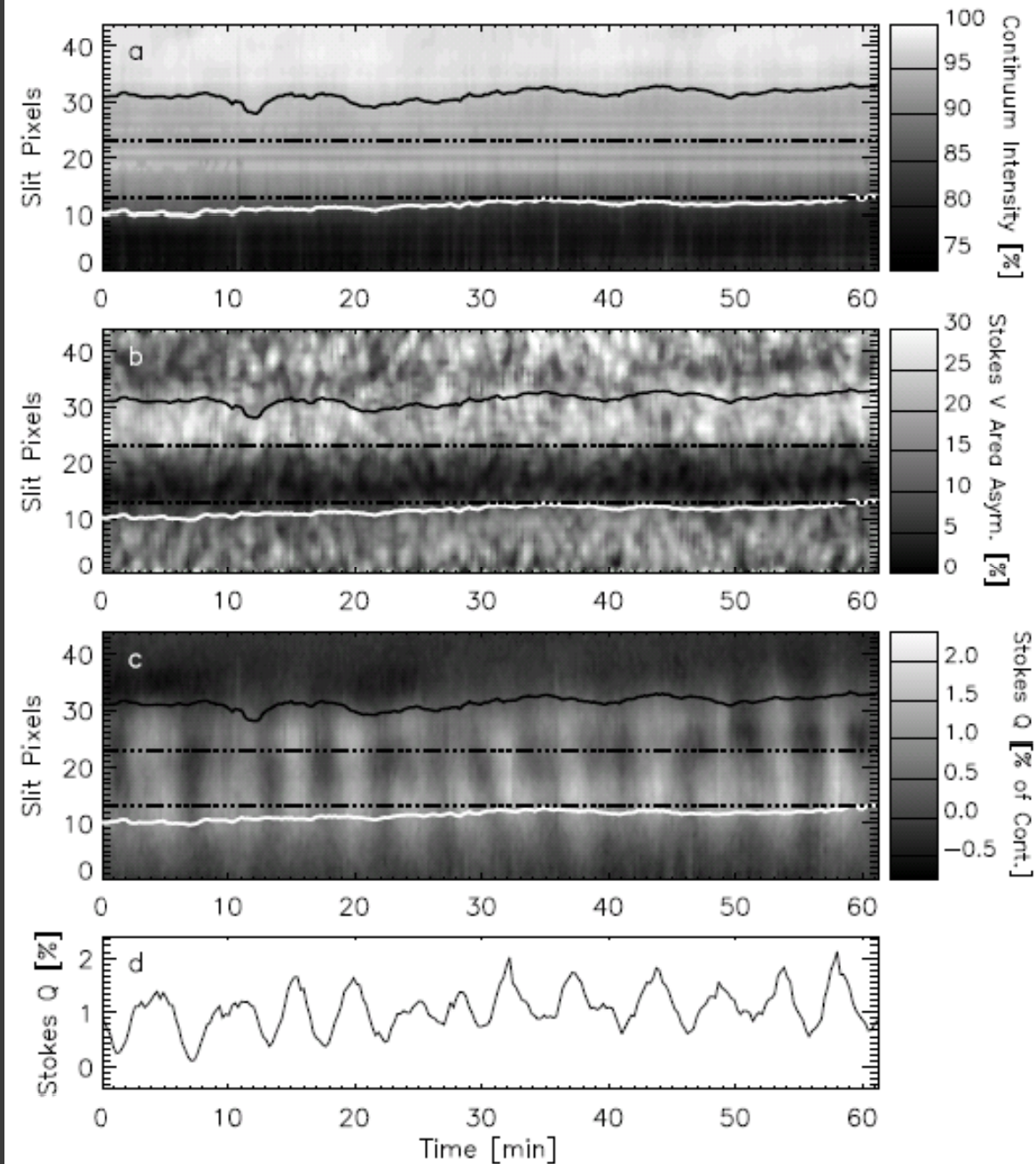


- SPINOR applied to:  
Fe I 15648 / 15652
- 1 magn. comp (4 nodes)  
1 straylight comp.
- molecular OH lines
- investigation of  
thermal-magnetic  
relation



# Penumbral Oscillations

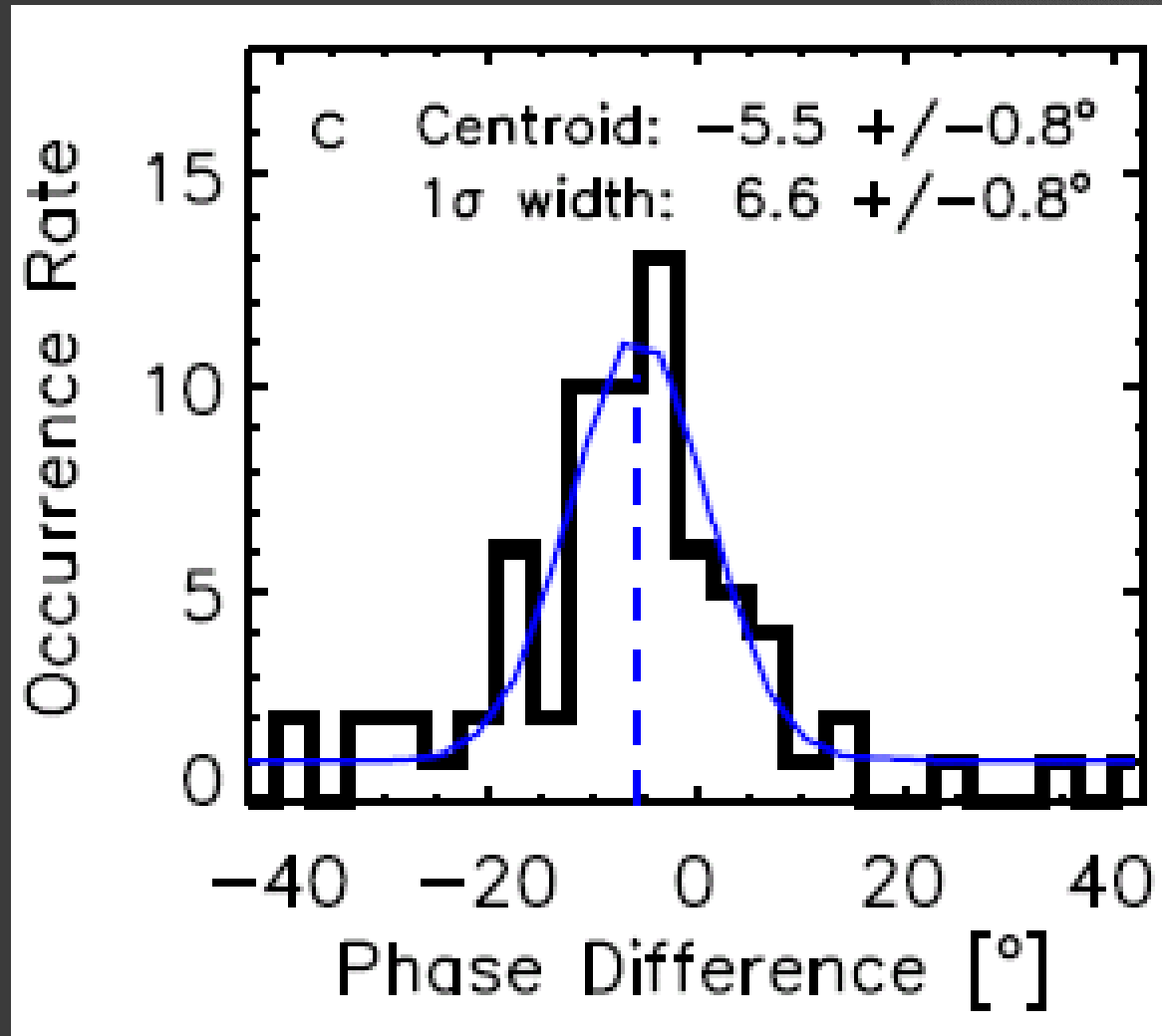
- oscillations observed in Stokes-Q of FeI 15662 and 15665
- calc. phase difference between Q-osc. → time delay
- 2-C inversion with straylight: → FT-component → magn. background
- RF-calc: difference in formation height (velocity): ~20 km
- relate time delay to speed of various wave modes



Bloomfield et al. [2007]

# Penumbral Oscillations

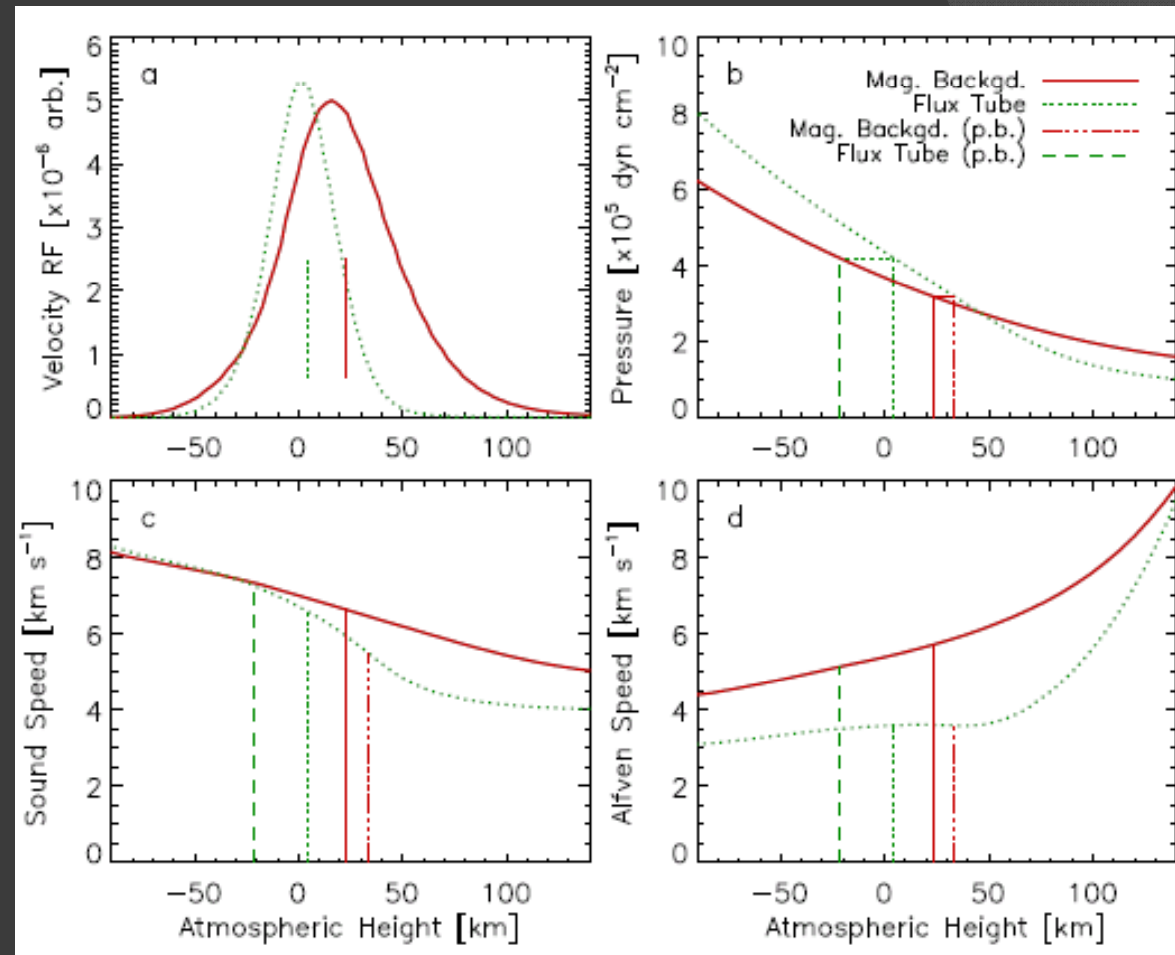
- oscillations observed in Stokes-Q of FeI 15662 and 15665
- calc. phase difference between Q-osc. → time delay
- 2-C inversion with straylight:
  - FT-component
  - magn. background
- RF-calc: difference in formation height (velocity): ~20 km
- relate time delay to speed of various wave modes



Bloomfield et al. [2007]

# Penumbral Oscillations

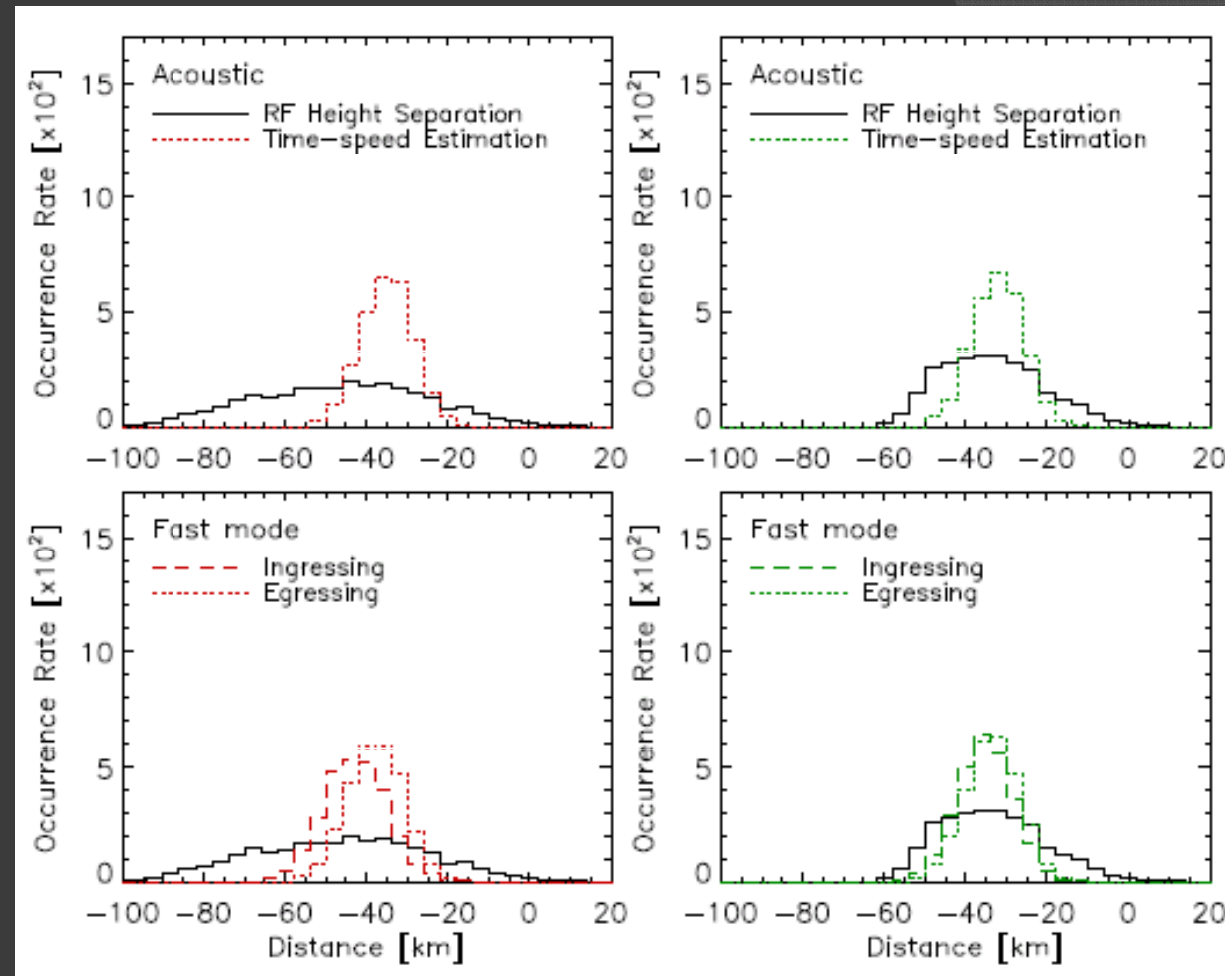
- oscillations observed in Stokes-Q of FeI 15662 and 15665
- calc. phase difference between Q-osc. → time delay
- RF-calc: difference in formation height (velocity): ~20 km
- 2-C inversion with straylight: → FT-component → magn. background
- relate time delay to speed of various wave modes



Bloomfield et al. [2007]

# Penumbral Oscillations

- oscillations observed in Stokes-Q of FeI 15662 and 15665
- calc. phase difference between Q-osc. → time delay
- 2-C inversion with straylight:  
→ FT-component  
→ magn. background
- RF-calc: difference in formation height (velocity): ~20 km
- relate time delay to speed of various wave modes



→ best agreement for:  
fast-mode waves  
propagating 50° to the vertical

Bloomfield et al. [2007]



Analysis of 51 umbral dots using SPINOR:

- 30 peripheral, 21 central UD
- nodes in  $\log(\tau)$ : -3,-2,-1,0 (spline-interpolated)
- of interest:
  - atomspheric stratification
    - $T(\tau)$ ,  $B(\tau)$ ,  $VLOS(\tau)$
    - INC, AZI,  $V_{MIC}$ ,  $V_{MAC}$  const.
- no straylight (extensive tests showed, that inversions did not improve significantly)

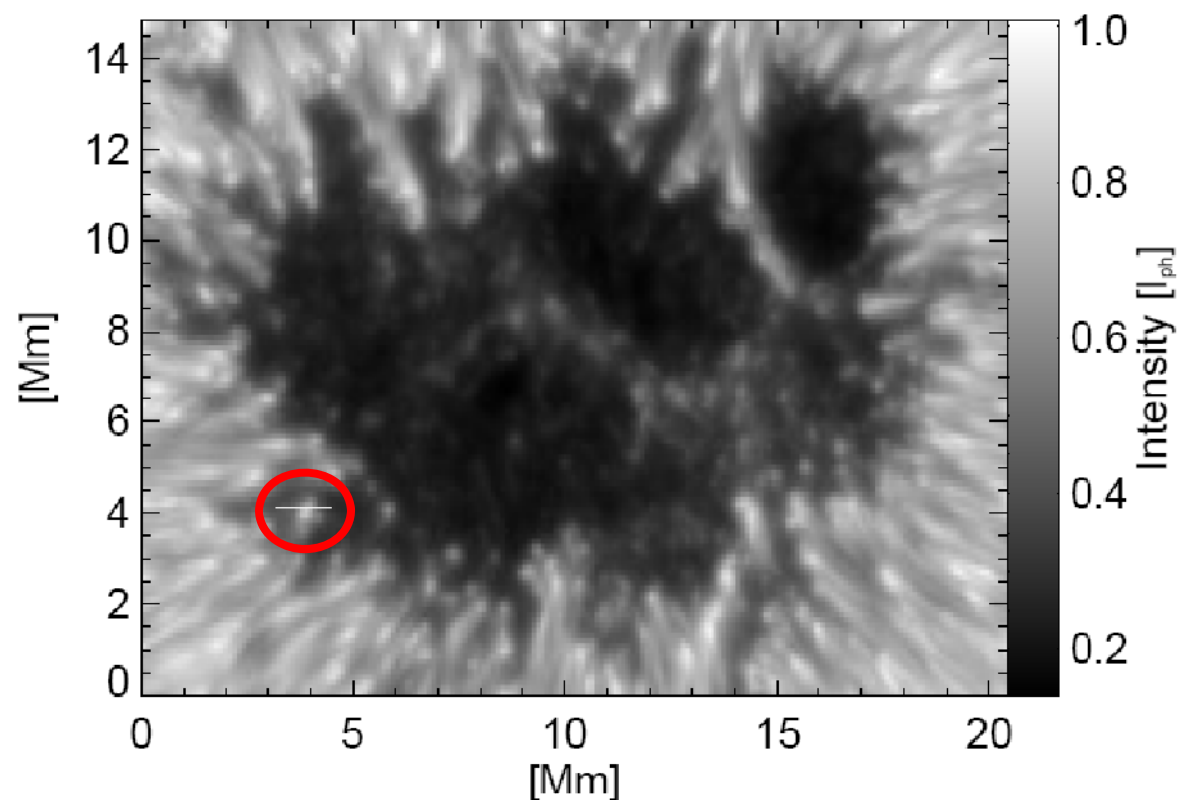
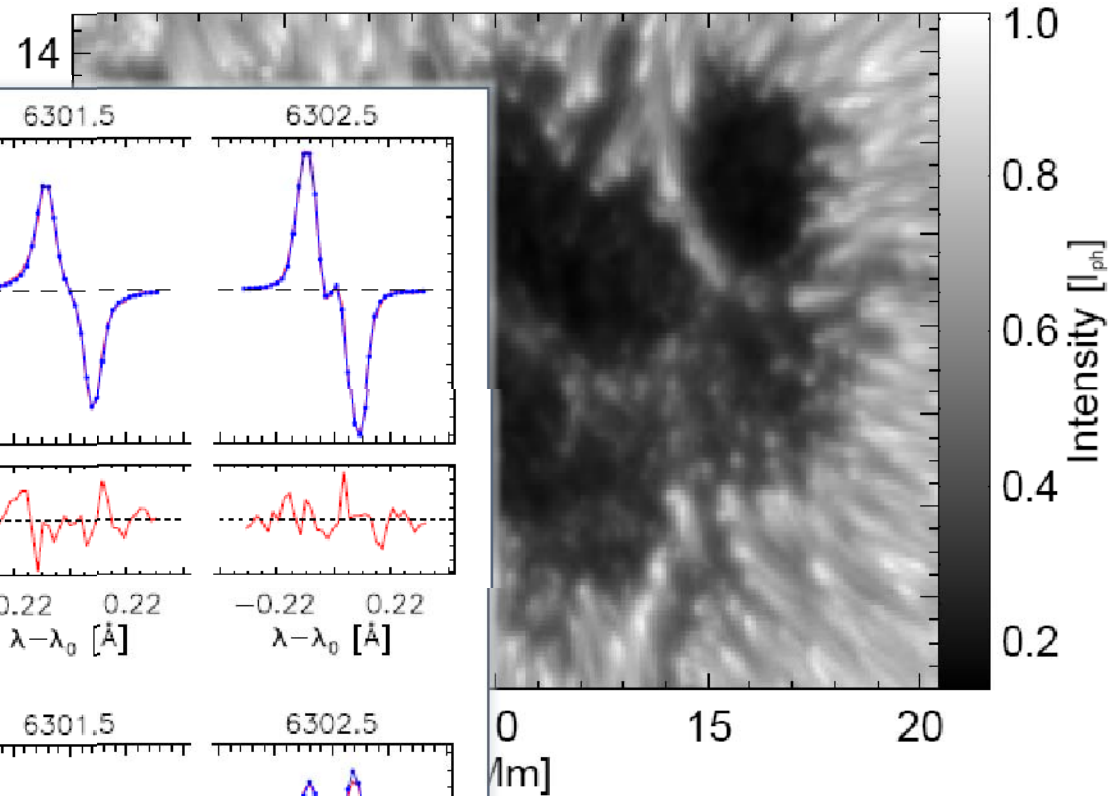
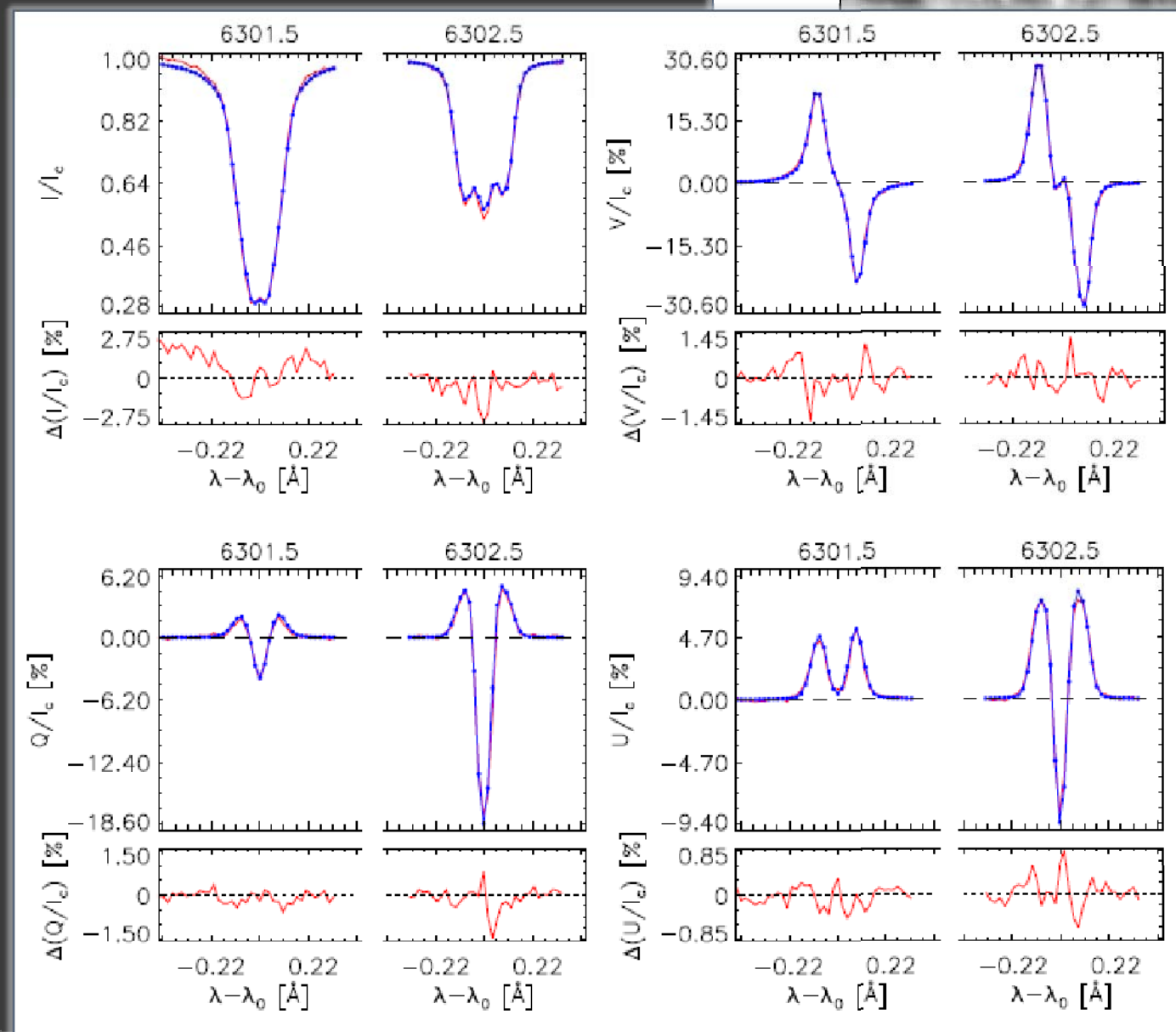


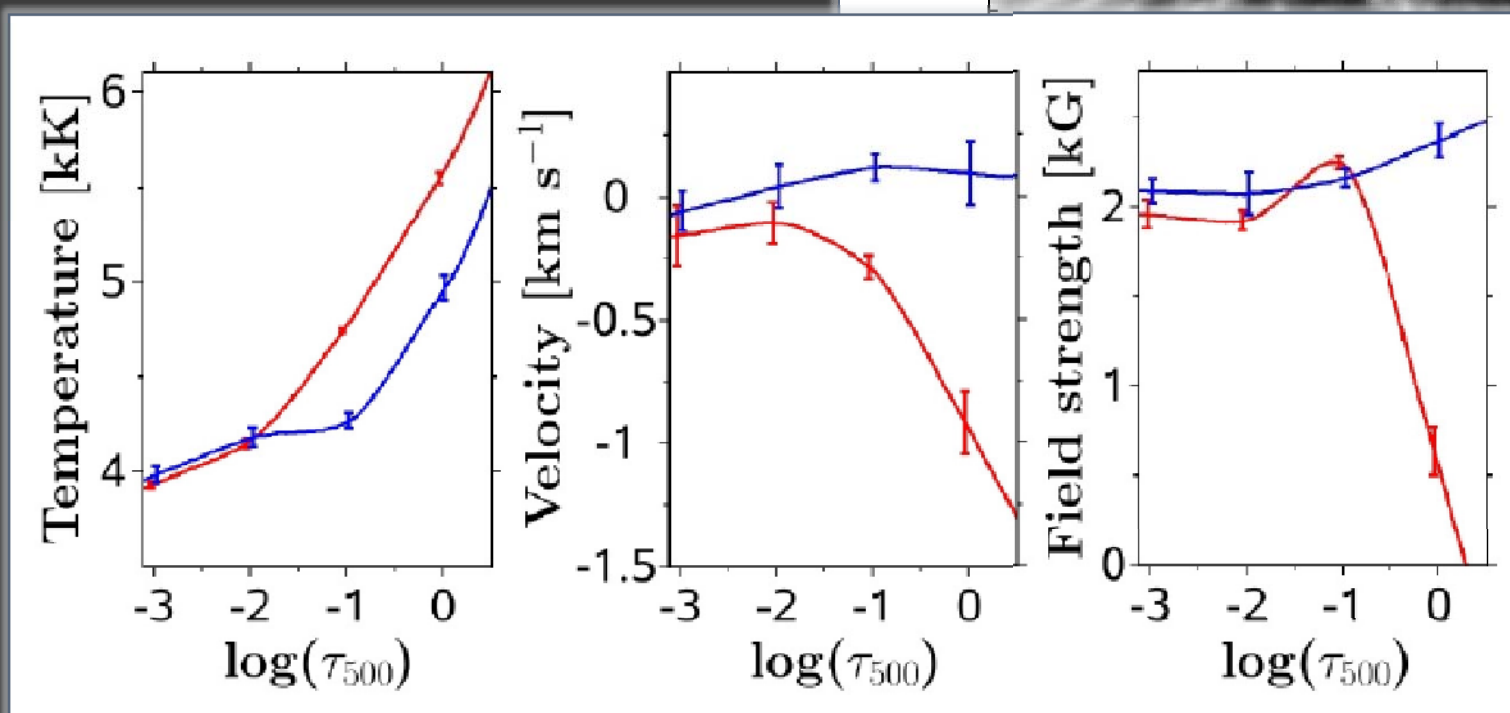
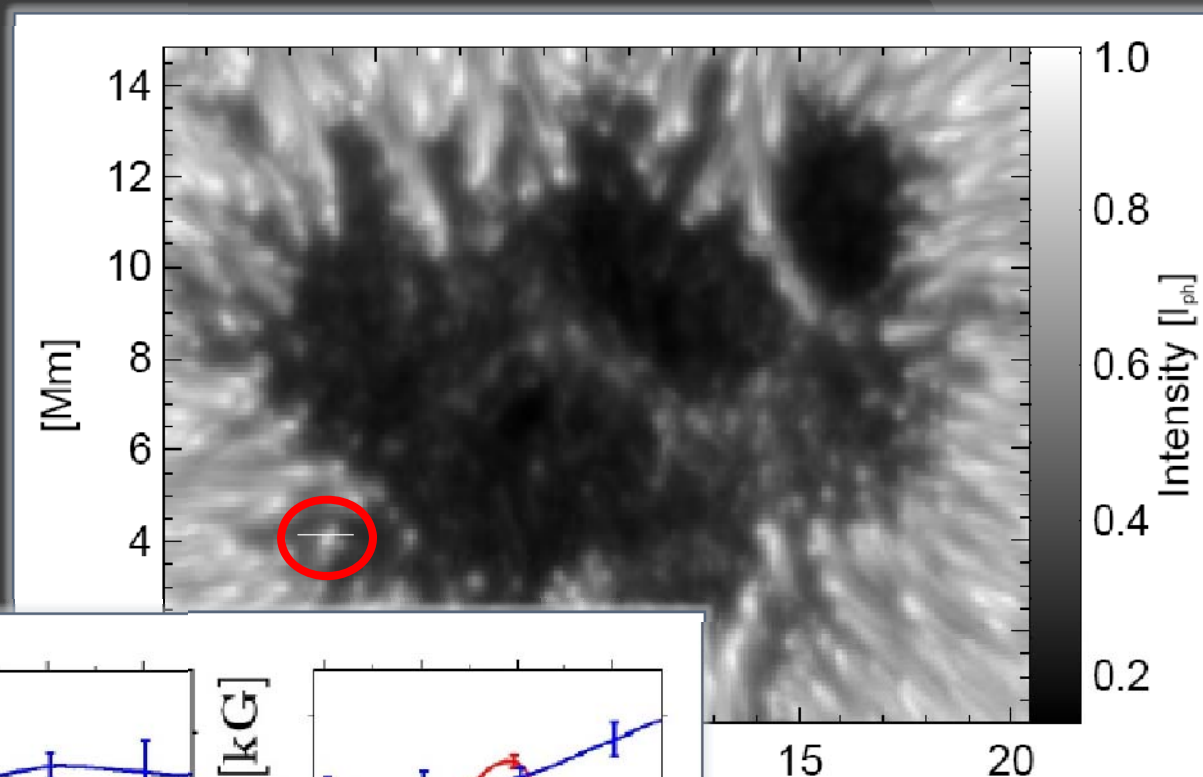
FIG. 1.— Continuum intensity map of the sunspot NOAA 10933 as observed by the *Hinode* SOT/SP on 2007 January 5. Heliocentric angle is  $\theta = 4^\circ$ . Intensities are normalized to the intensity level of the quiet photosphere  $I_{ph}$ . The white line at (4,4) Mm marks the cut through an umbral dot (UD) that is discussed in greater detail.

center of UD:



Intensity map of the sunspot NOAA 10933  $\Gamma$ /SP on 2007 January 5. Heliocentric velocity profiles are normalized to the intensity level of the penumbra. The white line at (4,4) Mm marks the location of the umbral dot (UD) that is discussed in greater detail in the text.

atmospheric stratification  
retrieved in center (red) and the  
diffuse surrounding (blue)



of the sunspot NOAA 10933  
in 2007 January 5. Heliocentral  
white line at (4,4) Mm marks  
that is discussed in greater

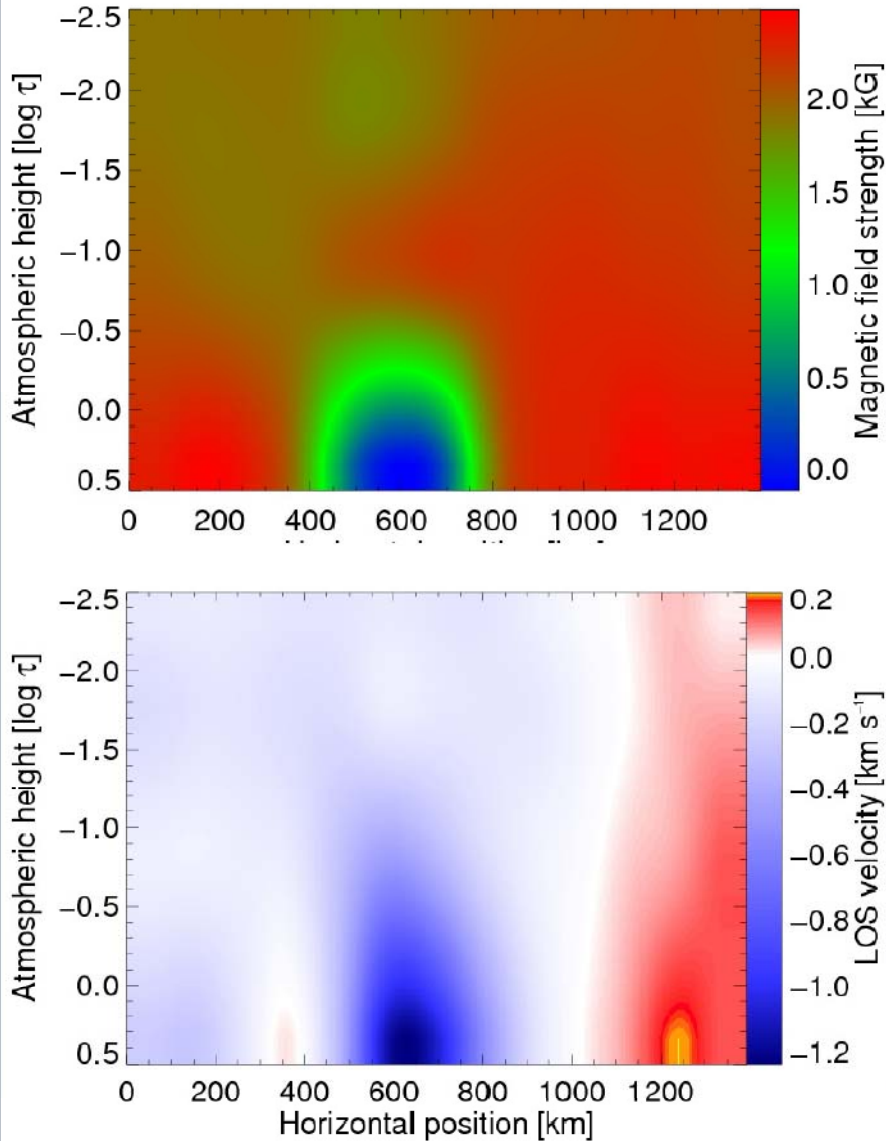


FIG. 5.— Vertical cut through the UD marked in Figure 1 in the direction indicated by the white line. Colors of the top panel indicate magnetic field strength. The bottom panel shows LOS velocity. Negative velocities are upflows.

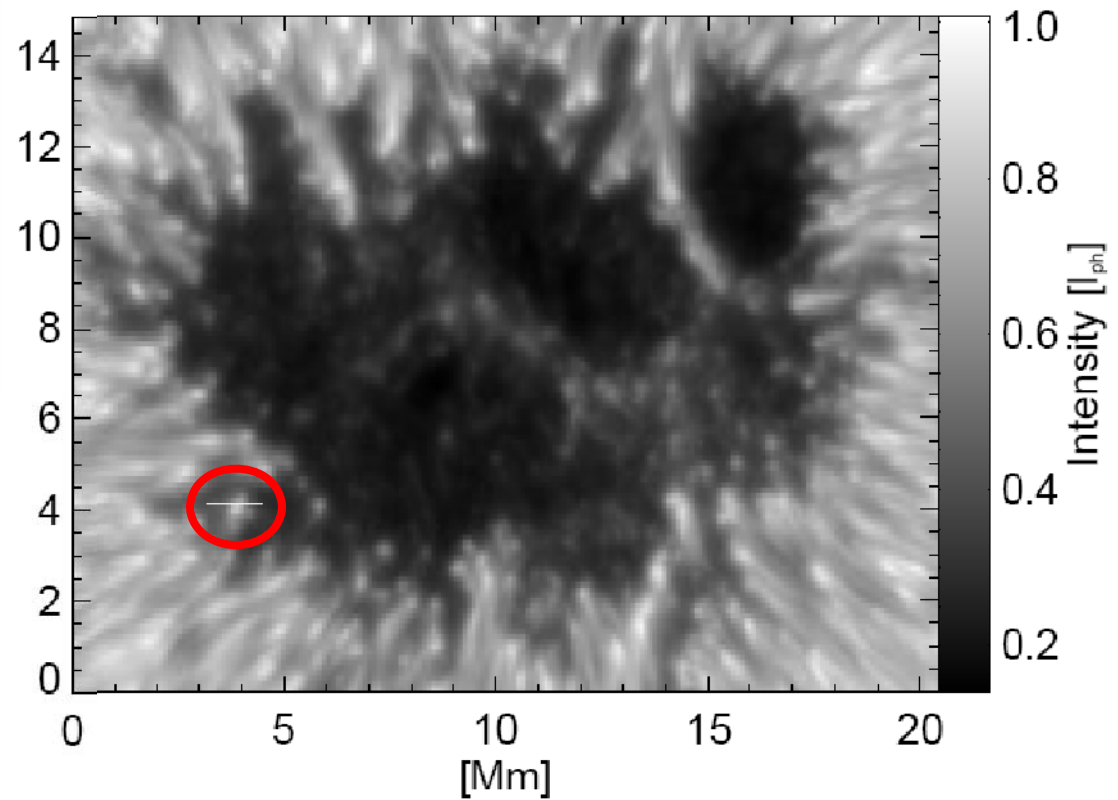


FIG. 1.— Continuum intensity map of the sunspot NOAA 10933 observed by the *Hinode* SOT/SP on 2007 January 5. Heliocentric angle is  $\theta = 4^\circ$ . Intensities are normalized to the intensity level of the quiet photosphere  $I_{ph}$ . The white line at (4,4) Mm marks the cut through an umbral dot (UD) that is discussed in greater detail in the next section.

## Vertical cut through UD

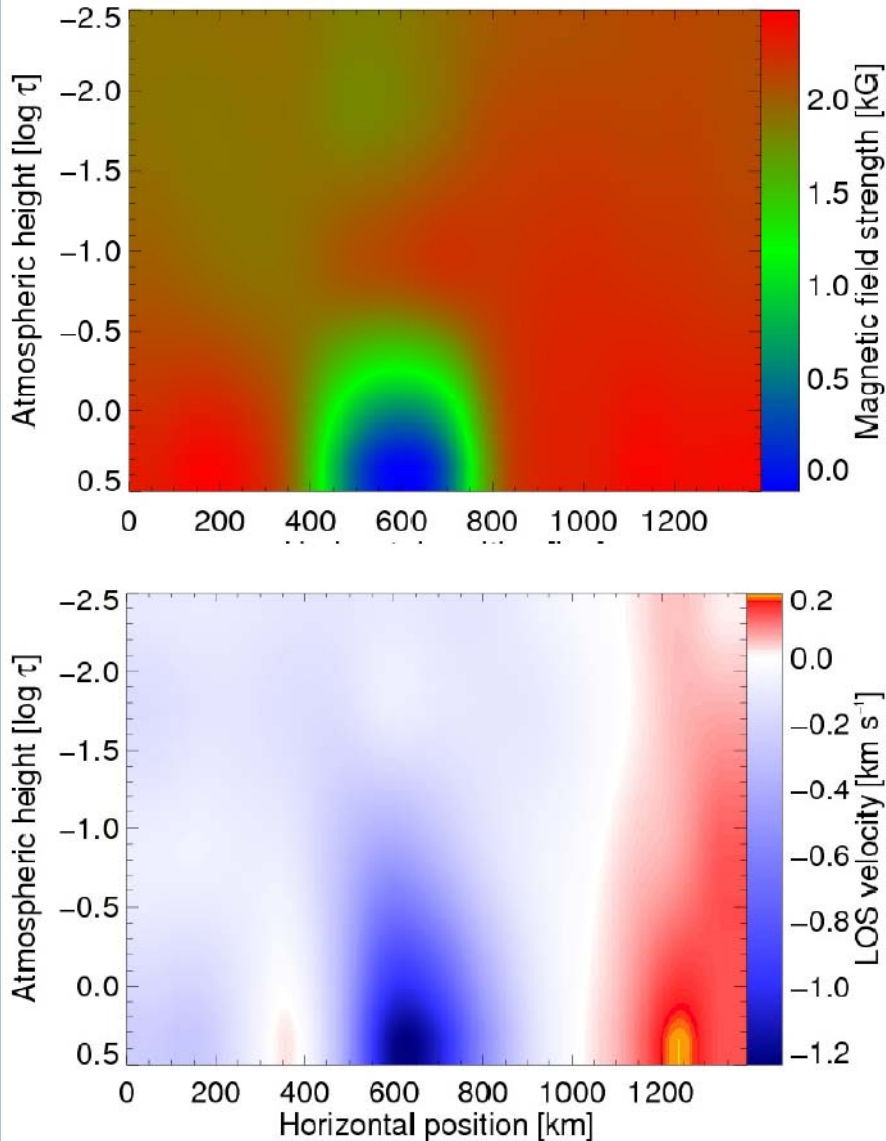


FIG. 5.— Vertical cut through the UD marked in Figure 1 in the direction indicated by the white line. Colors of the top panel indicate magnetic field strength. The bottom panel shows LOS velocity. Negative velocities are upflows.

## Conclusions:

- inversion results are remarkably similar to simulations of Schüssler & Vögler (2006)
- UDs differ from their surrounding mainly in lower layers
- T higher by  $\sim 550$  K
- B lower by  $\sim 500$  G
- upflow  $\sim 800$  m/s
- differences to V&S:
  - field strength of DB is found to be depth dependent
  - surrounding downflows are present, but not as strong and as narrow as in MHD (resolution?)

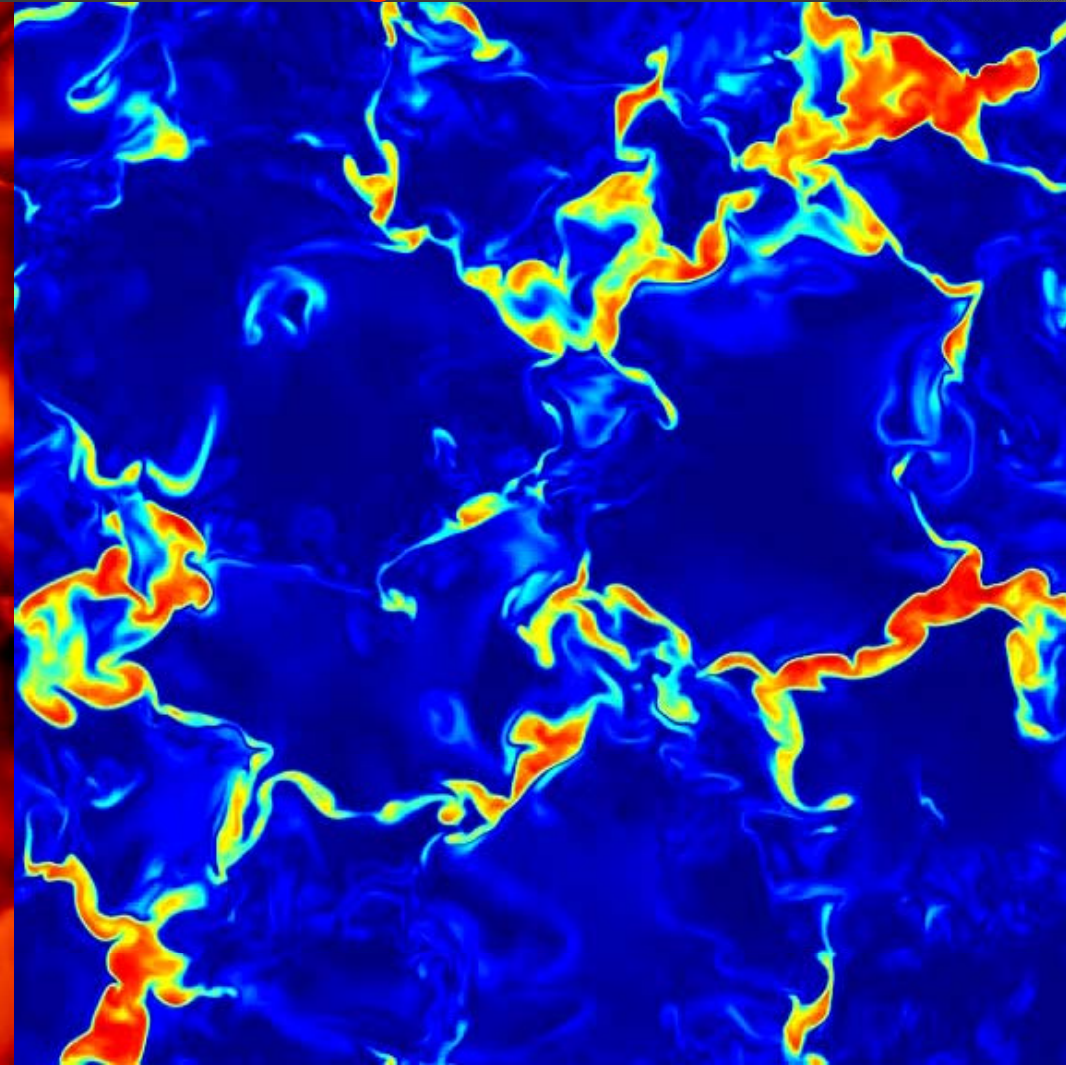
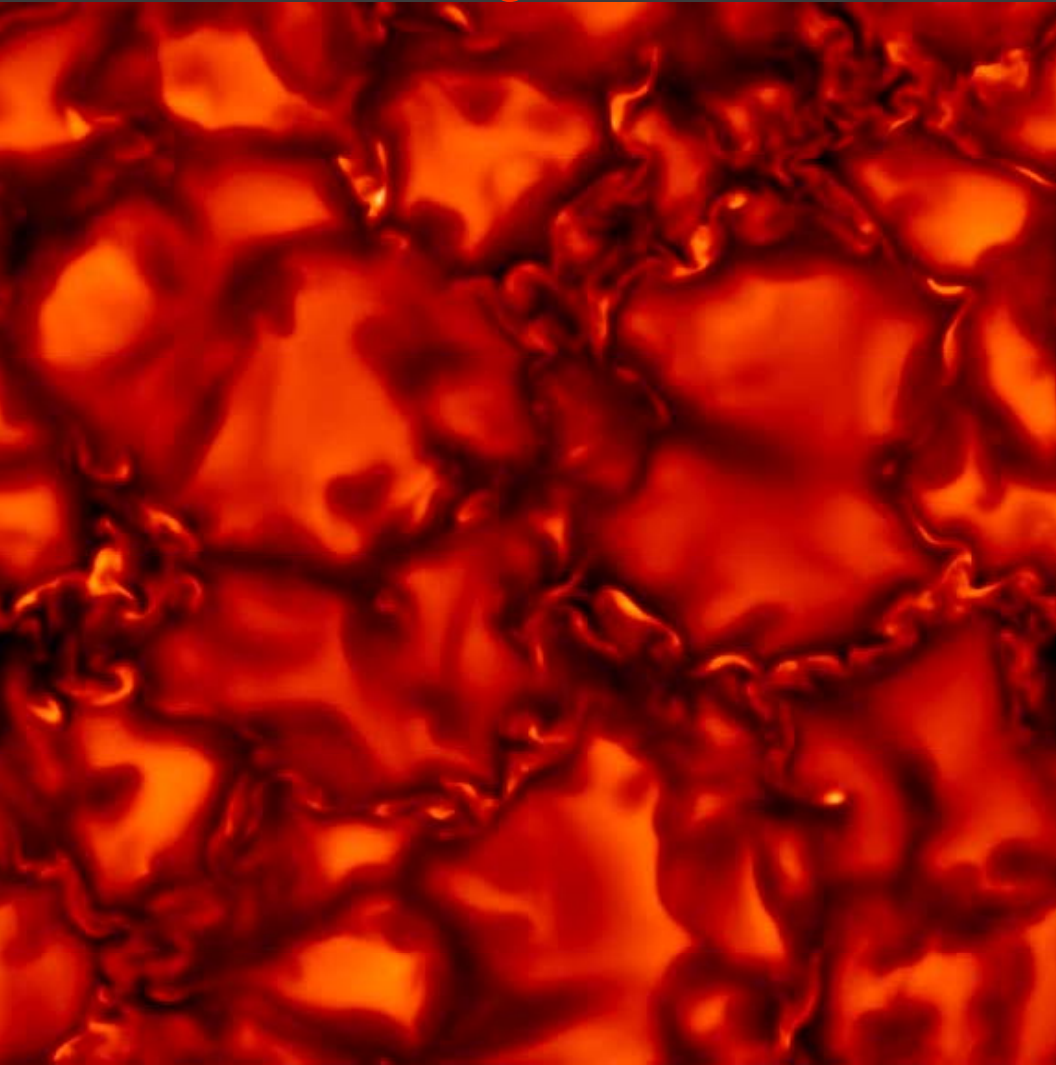
# Analysis of Hi-Res Simulations (forward calc.)

Vögler & Schüssler

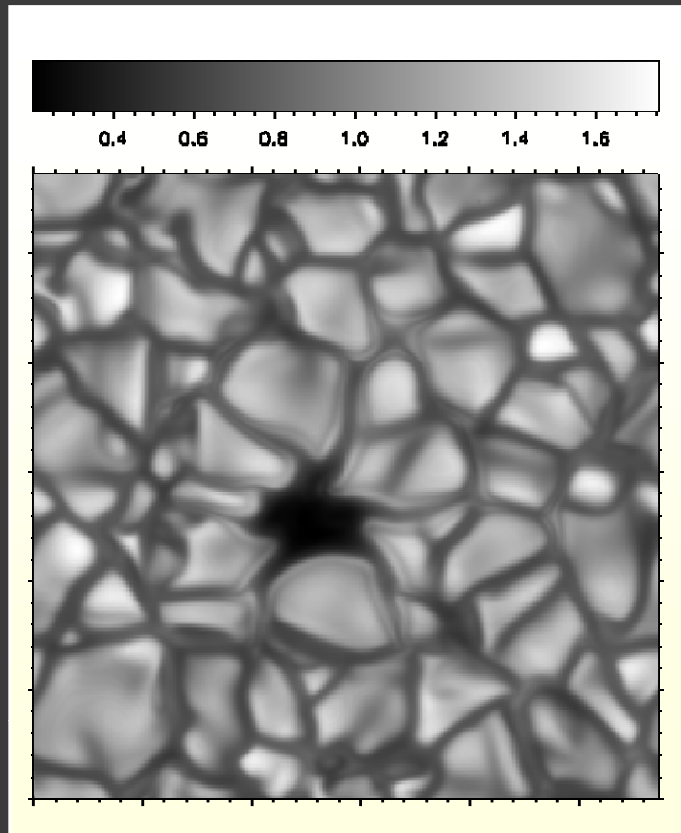
$\langle B_z \rangle = 200$  G; Grid: 576 x 576 x 100 (10 km horiz. cell size)

Brightness

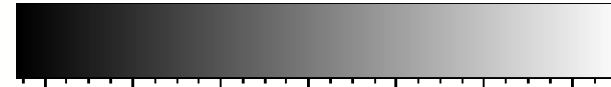
Magnetic field



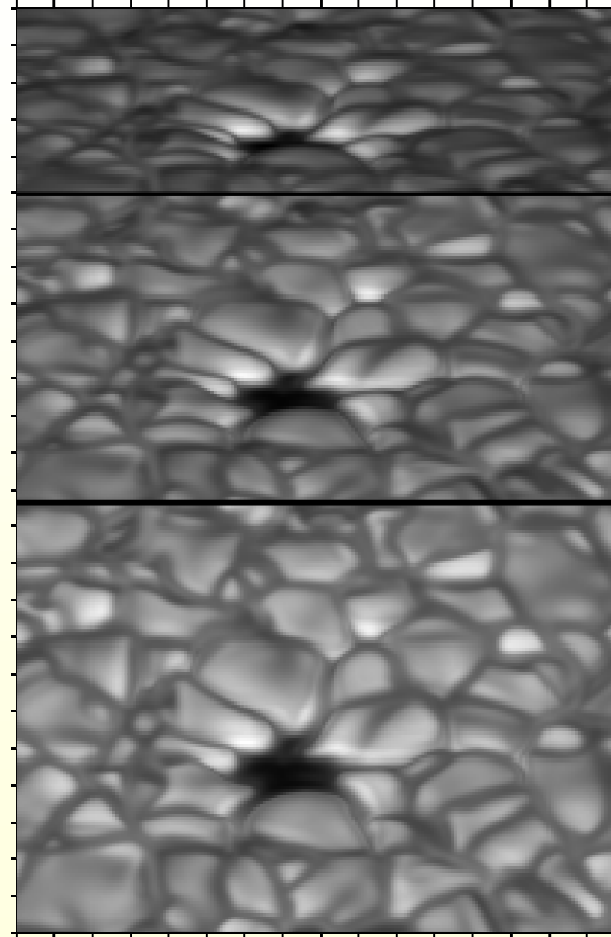
$\mu=1$



Intensity (normalized, 500nm)



0.2 0.4 0.6 0.8 1.0 1.2 1.4



$\mu=0.3$

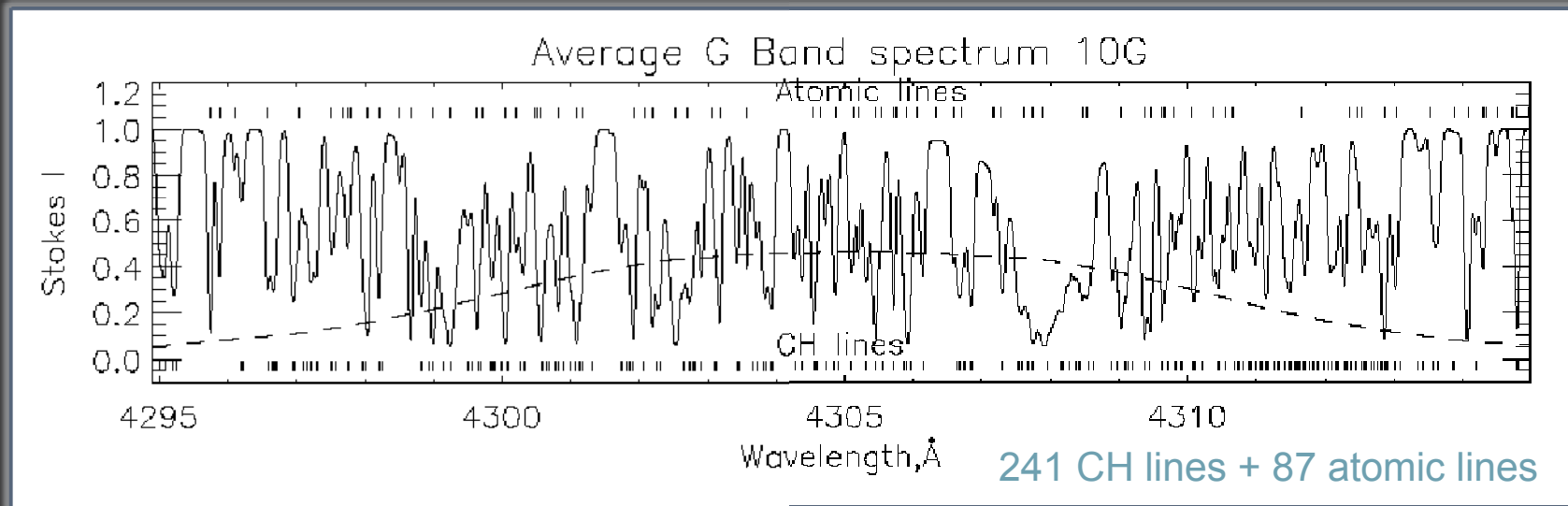
$\mu=0.5$

$\mu=0.7$

1''

# SPINOR: G-band spectrum synthesis

G-Band (Fraunhofer): spectral range from 4295 to 4315 Å contains many temperature-sensitive molecular lines (CH)



For comparison with observations, we define as G-band intensity the integral of the spectrum obtained from the simulation data:

$$I_G = \int_{4295 \text{ \AA}}^{4315 \text{ \AA}} I(\lambda) d\lambda$$

[Shelyag, 2004]



## Stopro & Spinor Introduction



Andreas Lagg · Max-Planck-Institut für Sonnensystemforschung · Katlenburg-Lindau, Germany

Download from <http://www.mps.mpg.de/homes/lagg>  
GBSO download-section → spinor  
use *invert* and *IR\$soft*

# Exercise IV

## SPINOR installation and basic usage



- install and run SPINOR
- atomic data file, wavelength boundary file
- use xinv interface
- SPINOR in synthesis (STOPRO)-mode
- 1<sup>st</sup> inversion:
  - Hinode dataset of HeI $\lambda$ 6678
- play with noise level / initial values / parameter range
- change  $\log(\tau)$  scale
- try to get the atmospheric stratification of an asymmetric profile
- invert HeI $\lambda$ 6678 synthetic profiles

Examples: <http://www.mps.mpg.de/homes/lagg>

→ Abisko 2009 → spinor → abisko\_spinor.tgz

unpack in spinor/inversions:

```
cd spinor/inversions ; tar xzf abisko_spinor.tgz
```